

Usnic Acid Targets 14-3-3 Proteins and Suppresses Cancer Progression by Blocking Substrate Interaction

Mücahit Varlı, Suresh R. Bhosle, Eunae Kim, Yi Yang, İsa Taş, Rui Zhou, Sultan Pulat, Chathurika D. B. Gamage, So-Yeon Park, Hyung-Ho Ha, and Hangun Kim*



Cite This: *JACS Au* 2024, 4, 1521–1537



Read Online

ACCESS |

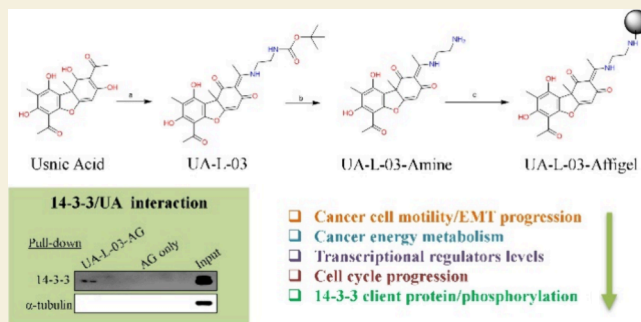
Metrics & More

Article Recommendations

Supporting Information

ABSTRACT: The anticancer therapeutic effects of usnic acid (UA), a lichen secondary metabolite, have been demonstrated *in vitro* and *in vivo*. However, the mechanism underlying the anticancer effect of UA remains to be clarified. In this study, the target protein of UA was identified using a UA-linker-Affi-Gel molecule, which showed that UA binds to the 14-3-3 protein. UA binds to 14-3-3, causing the degradation of proteasomal and autophagosomal proteins. The interaction of UA with 14-3-3 isoforms modulated cell invasion, cell cycle progression, aerobic glycolysis, mitochondrial biogenesis, and the Akt/mTOR, JNK, STAT3, NF- κ B, and AP-1 signaling pathways in colorectal cancer. A peptide inhibitor of 14-3-3 blocked or regressed the activity of UA and inhibited its effects. The results suggest that UA binds to 14-3-3 isoforms and suppresses cancer progression by affecting 14-3-3 targets and phosphorylated proteins.

KEYWORDS: usnic acid, lichen secondary metabolite, cancer, energy metabolism, target protein, 14-3-3



INTRODUCTION

Colorectal cancer is the third-most common cancer and the second leading cause of cancer-related death worldwide. The 5 year survival rate of CRC is 64%; however, for metastatic CRC, the 5 year survival is 12%, underscoring the need to develop new effective treatments for this disease.¹ The development of new targeted therapies has improved the clinical outcomes of CRC by providing potent therapeutic agents.² Although targeted therapies have been the object of research for many years, this concept was renewed and developed in recent years. Targeted therapies for the treatment of colon cancer can be designed to inhibit the migration, proliferation, and differentiation of cancer cells.^{3,4}

Usnic acid (UA), a lichen secondary metabolite, is commonly found in various species of *Alectoria* (Alectoriaceae), *Ramalina* (Ramalinaceae), *Usnea* (Usneaceae), *Evernia*, *Lecanora*, *Cladonia*, *Hypotrachyna*, and other lichen species.^{5–8} Comprehensive studies have been carried out to understand the beneficial effects of UA, and its antimicrobial, antiviral, and anticancer activities have been demonstrated.⁹ UA has been studied for its potential anticancer properties, such as inhibition of the cell cycle, cytotoxic effects, inhibition of angiogenesis suppresses of cell proliferation, and induction of apoptotic cell death in different cancer cell lines.^{10–14} Potassium usnate was developed as a water-soluble UA form to increase the bioavailability of UA, and its therapeutic potential for cancer treatment has been suggested.⁹

The 14-3-3 family of intracellular proteins is present in all eukaryotic species. The 14-3-3 proteins are a family of dimeric, well-conserved, α -helical phosphoserine/threonine binding proteins with a molecular weight of 28–33 kDa that regulate the activity of target proteins in multiple signaling pathways and affect many human diseases.^{15–18} A link between 14-3-3 expression levels and the development of colon cancer has been reported.¹⁹ In particular, 14-3-3 proteins regulate cell cycle progression, DNA damage, cell death, and cellular metabolism.^{20,21}

Humans have seven 14-3-3 isoforms (α/β , ϵ , γ , η , σ , τ , and δ/ζ) that act as scaffolds for regulatory phosphoproteins engaged in a variety of critical physiological activities.¹⁹ Nine α -helices form an amphipathic groove on each monomer, allowing it to bind to protein partners (most often phosphorylated proteins).¹⁹ The 14-3-3 protein interacts with many proteins and is thus considered a therapeutic target. Potential inhibitors and stabilizers of 14-3-3 protein–protein interactions have been reported in the literature.

Received: January 9, 2024

Revised: March 7, 2024

Accepted: March 19, 2024

Published: April 11, 2024



Fu et al. identified R18 as an inhibitor of 14-3-3 by phage display (protein database (PDB) ID: 1A38).^{22,23} The groups of Ottman and Grossmann showed that the ExoS macrocyclic peptide, which is derived from peptides containing the 14-3-3 binding motif, binds to 14-3-3- ζ and effectively inhibits protein interactions (PDB ID: 2O02, 4N84, and 5J31).²⁴ 14-3-3- σ binds directly to Tau, a target for the treatment of Alzheimer's disease, via the Ser214 and Ser324 residues (PDB ID: 4FL5, 4Y32, and 4YSI).^{25–27} Yao et al. used the small molecule microarray technique to develop inhibitors of 14-3-3 protein interactions (2-5, Prodrug 15, and 19a).^{28,29} Botta et al. identified BV01, BV02, BV101, and compound 9 as inhibitors of 14-3-3- σ protein interactions by pharmacopoeia grounding, library design, virtual screening, and organic synthesis. BV02 is an inhibitor of the interaction between 14-3-3- σ and cAbl in chronic myeloid leukemia.^{30–33} HSP20 Compound 85070 modulates the interaction between phosphorylated HSP20 and the 14-3-3 proteins. The functional effects and underlying mechanism of this molecule remain to be fully elucidated.³⁴ The small molecule FOBISIN101 is a covalent 14-3-3 inhibitor developed by Fu et al. The X-ray structure showed that FOBISIN101 binds to 14-3-3- ζ and inhibits Raf1 interactions (PDB ID: 3RDH).^{35,36} Imoto et al. showed that the natural product moverastin, derived from *Aspergillus*, inhibits cancer cell migration.³⁷ The moverastin derivative UTKO1 inhibits the migration of human esophageal tumor cells.³⁸ A biotinylated derivative of UTKO1 was developed to search for binding proteins, resulting in the identification of 14-3-3- ϵ and ζ isoforms as potential target proteins.^{39,40} The therapeutic effects of UTKO1 were demonstrated in experiments with seven isoforms of 14-3-3, which showed that UTKO1 binds the 14-3-3- ζ isoform to the C-terminal domain.^{24,37–39} Phosphonate-type inhibitors of 14-3-3 bind to 14-3-3- σ , and docking results show that it binds to many protein residues (PDB ID: 4DHT).^{28,41,42} Bier et al. reported an inhibitor containing phosphate called “molecular tweezers”, which inhibit the binding of nonphosphorylated ExoS and Raf to 14-3-3- σ by binding to the Lys214 residue (PDB ID: 4HQW and 4HRU).⁴³ Fusicoccin A is a diterpene glycoside produced by the phytopathogenic fungus *Phomopsis amygdali*.⁴⁴ The mechanism by which the plasma membrane forms a binary complex between the regulatory domain H⁺-ATPase and 14-3-3 adapter proteins was reported.⁴⁵ Semisynthetic analogs of fusicoccane have been developed as stabilizers of 14-3-3 that act as a “molecular glue”.^{46–48} Epibestatin, pyrrolidone1, and pyrazole34 are 14-3-3 stabilizers developed in 2010. Pyrrolidone1 and pyrazole34 stabilize the interaction between 14-3-3 and PMA2 (PDB ID: 3MS1).^{49,50} Uyeda et al. reported that adenosine monophosphate stabilizes the complex of 14-3-3 and ChREBP (carbohydrate response element binding protein), and binding points on 14-3-3- β are shown by docking results (PDB ID: 5F74).⁵¹ In the current study, we identified the 14-3-3 protein as a target of UA involved in the effect of UA on cell cycle arrest and cell motility, providing insight into the mechanism underlying the anticancer effects of UA. The effects of UA on cell metabolism were also examined.

MATERIALS AND METHODS

Cell Culture and Reagents

Colon cancer cell lines CaCo2 (microsatellite stable (MSS) and wild-type KRAS, BRAF, and PIK3CA) and HCT116 (KRAS mutation) were used in this study.⁵² HEK293T cells were also used in the reporter assay. Cells were cultured in Dulbecco's modified Eagle's medium

supplemented with 10% fetal bovine serum and 1% penicillin–streptomycin solution in a 37 °C incubator under a humidified atmosphere containing 5% CO₂. Brefeldin A (Al), chloroquine (CQ), a proteasome inhibitor MG132, and 3-methyladenine (3-MA) (Sigma) were administered at the indicated concentrations.

Plasmids and Luciferase Reporter Assay

Plasmids are given in Supplementary Table S1. Lipofectamine LTX with PLUS reagents were used for transfection of 14-3-3 isoforms, sc138, and sc174 into cancer cells. For the reporter assay, HEK293T was plated in a 24-well plate, left to attach, and then transfected with 100 ng of reporters (STAT3-luc,⁵⁵ AP1-luc,⁵⁶ and NF- κ B-luc⁵⁵ plasmid) and 100 ng of 14-3-3 isoform plasmids or sc138 along with 2 ng of Renilla-luc (pRL-TK) plasmid. Transfections were performed using the X-treme GENE 9 DNA transfection reagent (Roche, Werk Penzberg, Germany). Twenty-four hours after transfection, cells were treated with usnic acid or DMSO and incubated for 48 h at 37 °C under 5% CO₂. To control for transfection efficiency, luciferase activity was normalized against Renilla activity using the Dual-Luciferase reporter assay system (Promega, Madison, WI, USA).

Invasion Assay

Cell invasion was assessed by using Boyden chambers coated with 1% gelatin. A total of 5×10^4 CaCo2 and HCT116 cells in 100 μ L DMEM containing 0.2% bovine serum albumin (BSA) were plated onto precoated inserts and incubated with UA or UA-linker or DMSO for 24 h. The lower chamber was filled with 600 μ L of DMEM containing 0.2% BSA and 10 μ g/mL fibronectin (EMD Millipore Corp., Billerica, MA, USA) as a chemoattractant. After incubation, cells in the upper chamber were fixed and stained using a Diff-Quick kit (Sysmex, Kobe, Japan).⁵⁷

Synthesis of UA-L-03

To a solution of *tert*-butyl(2-aminoethyl)carbamate (0.139 g, 0.87 mmol, 1 equiv) in absolute ethanol was slowly added usnic acid (0.300 g, 0.87 mmol, 1, equiv) at RT under the nitrogen gas. Then, the reaction mixture was stirred at 80 °C for 4 h. The reaction progress was monitored by checking TLC. After completion of the reaction, the reaction mixture was concentrated under reduced pressure. Purification by column chromatography on silica gel gave the protected compound (UA-L-03) as a white solid. Yield (0.305, 77%). R_f (0.3). ¹H NMR (400 MHz, CDCl₃) δ 13.36 (s, 1H), 11.92 (s, 1H), 5.79 (s, 1H), 4.87 (s, 1H), 3.65 (t, J = 5.5 Hz, 2H), 3.42 (q, J = 6.1 Hz, 2H), 2.68 (s, 3H), 2.65 (s, 3H), 2.10 (s, 3H), 1.71 (s, 3H), 1.45 (s, 9H). ¹³C NMR (400 MHz, CDCl₃) δ 200.7, 163.6, 158.3, 155.9, 108.2, 105.1, 101.5, 77.4, 77.1, 76.8, 43.6, 32.0, 31.4, 28.4, 18.4, 7.6. MS (ESI+, m/z): 485 [M + H].

Synthesis of (*E*)-6-Acetyl-2-(1-((2-aminoethyl) amino) ethylidene)-7,9-dihydroxy-8,9b-dimethyldibenzo[b,d]-furan-1,3(2*H*,9*bH*)-dione (UA-L-03 Amine)

To a solution of UA-L-03 (0.300 g, 0.61 mmol, 1 equiv) dissolved into anhydrous DCM was slowly added TFA (1 mL) at 0 °C. The reaction mixture was transferred at room temperature and stirred for 2 h. After completion of the reaction, the solvents were evaporated and dried under high vacuum. Then, the compound was kept for recrystallization overnight into acetonitrile. After 12 h, a white crystal form was filtered from it, which gave a white compound (R_f = 0.1, 15% MeOH/DCM). ¹H NMR (400 MHz, DMSO-*d*₆) δ 13.42 (s, 1H), 12.95 (s, 1H), 12.24 (s, 1H), 7.90 (s, 2H), 5.92 (d, J = 1.8 Hz, 1H), 3.79 (s, 2H), 3.11 (t, J = 6.4 Hz, 2H), 2.64 (s, 3H), 2.60 (s, 3H), 1.97 (s, 3H), 1.66 (s, 3H). MS (ESI+, m/z): 385 [M + H].

General Procedure for Usnic Acid-Immobilized Affi-Gel-10

Affi-Gel-10 was transferred to a 3 mL cartridge with a polyethylene frit. The supernatant solvent was drained, and the Affi-Gel was washed with DMSO. A solution of the free-amine linker version of UA-L-03-amine in DMSO and DIEA was added to the gel. The cartridge was shaken well for 4 h at RT. The resulting slurry was drained, and the gel was washed with DMSO. The loading level (90%) was determined by analyzing the eluent mixed with an internal standard by LCMS and comparing the result to the initial reaction mixture. A solution of ethanolamine in DMSO and DIEA was added to the reaction cartridge

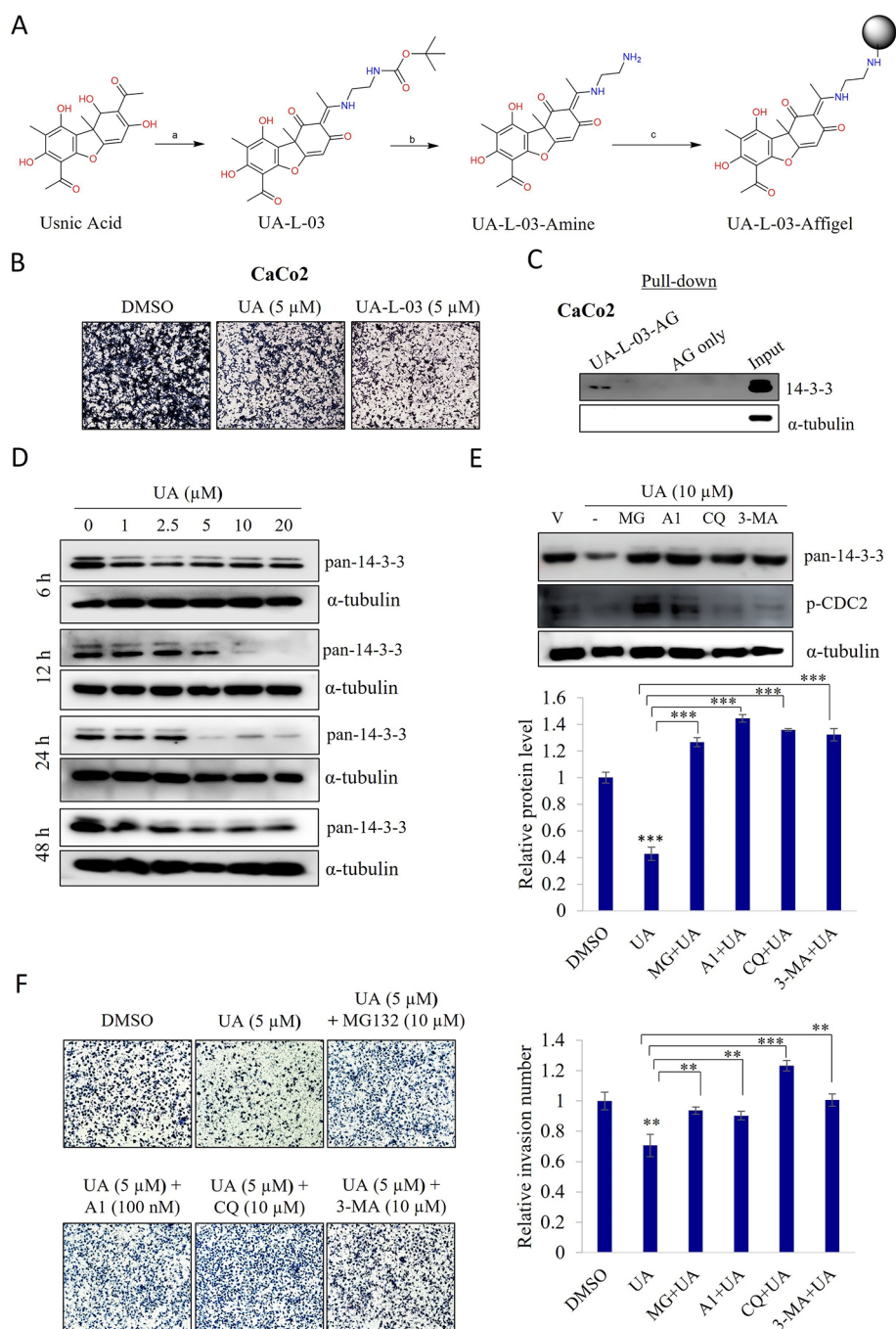


Figure 1. Identification of UA's binding protein. (A) Preparation of the usnic acid (UA)-Affi-Gel-linker. Synthesis of UA-L-03-immobilized Affi-Gel-10: (a) absolute ethanol, reflux, 4 h, RT, 12 h. (b) Trifluoroacetic acid (TFA), dichloromethane (DCM), 0 °C, RT, 2 h. (c) Affi-Gel-10, DMSO, RT, 4 h. (B) The UA-Affi-Gel-linker compound (UA-L-03), which was prepared to bind to the target proteins of UA, suppressed cell invasion by maintaining the activity of UA. A cell suspension containing 5×10^4 CaCo2 cells in medium containing 0.2% BSA was subjected to Transwell invasion assays. Cells were treated with 5 μ M UA for 24 h. (C) Identification of 14-3-3 proteins by analysis of proteins pulled down by the chemical probe. The CaCo2 cell lysate was incubated with the chemical probe, synthesized as described, to pull down binding proteins. Proteins were identified by immunoblot analysis using a pan-14-3-3 antibody. (D) Treatment with UA at different concentrations (1–20 μ M) and times (6–48 h) downregulated 14-3-3 protein levels in CaCo2 cells. UA downregulated 14-3-3 proteins by inducing proteasomal and autophagic degradation. (E) CaCo2 cells were pretreated with DMSO, the proteasome inhibitor MG132 (MG, 10 μ M), the lysosomal degradation inhibitors bafilomycin A1 (A1, 100 nM) and chloroquine (CQ, 10 μ M), or the autophagosome blocker type III phosphatidylinositol 3-kinase inhibitor (3-MA, 10 μ M) and later treated with 10 μ M UA. The levels of 14-3-3 proteins and p-CDC2 were examined by immunoblotting. Anti-p-CDC2 was used as the positive control, and α -tubulin was the loading control. Values are presented as arbitrary units of densitometry corresponding to signal intensity. * p < 0.05; ** p < 0.01; *** p < 0.001. (F) Effect of MG132, A1, CQ, and 3-MA on the suppression of cell invasiveness by UA. CaCo2 cells were treated with UA (5 μ M, 24 h) and pretreated with MG132 (10 μ M), A1 (100 nM), CQ (10 μ M), and 3-MA (10 μ M) for 12 h before being harvested and subjected to invasion assays. Data are presented as the mean \pm standard deviation. * p < 0.05; ** p < 0.01; *** p < 0.001.

and shaken well for 3 h at RT. The resulting slurry was drained, and the gel was washed with DMSO, water, and 2% sodium azide in water. The affigel product was stored in a 2% sodium azide solution in water at 4 °C.

Identification of the Cell Target of Usnic Acid

Usnic acid beads and control beads were incubated with the whole cell lysates of CaCo2 cells for 12 h at 4 °C and thoroughly washed six times with washing buffer (50 mM HEPES, 30 mM NaCl, 1 mM EDTA, 2.5 mM EGTA, 0.1% Tween-20, cocktail inhibitor, pH 7.5). To find the target that interact with UA, matrix-assisted laser desorption/ionization time-of-flight mass spectrometry was utilized.

Pulldown Assay

UA bead was incubated with CaCo2 cell lysates in pulldown buffer (50 mM HEPES, 30 mM NaCl, 1 mM EDTA, 2.5 mM EGTA, 0.1% Tween-20, cocktail inhibitor, pH 7.5) at 4 °C for 12 h. Beads were washed thoroughly using wash buffer (pulldown buffer), and bead-bound proteins were resolved on SDS-PAGE followed by immunoblot analysis with antibodies. Antibodies were detected with horseradish peroxidase-conjugated secondary antibody (Thermo Fisher Scientific, Waltham, MA, USA) using the Immobilon Western Chemiluminescent HRP Substrate Kit (Merck Millipore, Billerica, MA, USA) and imaging.

Western Blotting

Cells were treated with UA for the indicated experimental design, after which the protein extracted was separated by applying sodium dodecyl sulfate-polyacrylamide gel electrophoresis. For each sample, bands were measured by Multi-Gauge 3.0 and normalized against that of α -tubulin, β -actin, or GAPDH. Values were expressed as arbitrary densitometric units corresponding to signal intensity. Antibody information was given in [Supplementary Table S2](#).

Quantitative Real-Time PCR

Total RNA was isolated from CRC cells using RNAiso Plus (TaKaRa, Otsu, Japan) according to the manufacturer's instructions. A total of 1 μ g of RNA was converted into cDNA using M-MLV reverse transcriptase (Invitrogen, Carlsbad, CA, USA). Relative gene expression was analyzed using SYBR Green (Ezymomics, Seoul, Korea). The primers used for real-time PCR are listed in [Supplementary Table S3](#). Real-time PCR was performed, and data were analyzed using CFX (Bio-Rad, Hercules, CA, USA).

Flow Cytometry Analysis

Cells were seeded in six-well plates at a density of 2×10^5 cells/well, cultured overnight, treated with UA or DMSO for 24 or 48 h, trypsinized, and washed with a FACS wash solution. A trypsin solution was added and incubated for 10 min. After that, an RNase inhibitor was added and incubated for 10 min at room temperature. Samples were centrifuged, and the supernatants were removed. Pellets were resuspended in 100 μ L of 4 mg/mL PI (Sigma-Aldrich, St. Louis, MO, USA) and incubated for 2 h in the dark at 4 °C. Flow cytometry was performed with a CytoFLEX instrument (Beckman Coulter Life Sciences).⁵⁸

Seahorse Assay

To measure real-time changes in the extracellular acidification rate (ECAR) and oxygen consumption rate (OCR), an XF96 extracellular flux analyzer (Agilent, Santa Clara, CA, USA) was used. CRC cells were seeded at 1×10^4 cells/well, incubated overnight in a culture medium, and then treated with UA for 48 h. The plated cells were washed and loaded with 180 μ L of assay media enhanced with glucose, sodium pyruvate, and glutamine on the day of analysis. While incubating the cells for 60 min at 37 °C in a non-CO₂ incubator prior to analysis, 0.5 μ M rotenone (Rot) + antimycin A (AA) and 50 mM 2-deoxy-D-glucose (2-DG) were loaded into the hydrated sensor cartridge for ECAR analysis (glycolytic rate assay) and 1 μ M oligomycin, 1 μ M carbonyl cyanide 4-(trifluoromethoxy) phenylhydrazone (FCCP), and 0.5 μ M rotenone (Rot) + antimycin A (AA) were loaded for OCR analysis (Cell Mito Stress Test). OCR and ECAR were measured on a Seahorse XF instrument (Agilent).

Statistical Analysis

Statistical analyses were carried out using Sigma Plot 12.5 software (RRID:SCR_003210, Systat Software, Erkrath, Germany). Statistical significance between two groups was compared using Student's *t* test.

RESULTS

Usnic Acid Binds to 14-3-3 Proteins

To identify proteins modulated by UA, we developed a linker-bound UA (UA-linker-Ac) using Affi-Gel beads ([Figure 1A](#)). Cell invasion was examined to determine the activity of the linked UA, which showed that the UA-linker preserves the activity of UA ([Figure 1B](#)). Matrix-assisted laser desorption/ionization time-of-flight mass spectrometry (MALDI-TOF MS) was used to identify proteins that interact with UA. The interactions were confirmed using pull-down experiments with the UA-linker-Affi-Gel beads, control (Affi-Gel only), and CaCo2 cell lysates, which were detected with a pan 14-3-3 antibody. The results showed that UA binds to 14-3-3 proteins ([Figure 1C](#)). The mRNA expression levels of 14-3-3 isoforms were analyzed in colon cancer (COAD) samples and nontumor tissues using the GEPIA web tool. The results showed that all 14-3-3 isoforms are overexpressed in colon cancer. 14-3-3- β , 14-3-3- ϵ , 14-3-3- σ , 14-3-3- ζ , 14-3-3- α (phosphorylated form of 14-3-3- β), and 14-3-3- δ (phosphorylated form of 14-3-3- ζ) were significantly overexpressed in colon cancer tissues and associated with poor survival ([Supplementary Figure S1](#)).

Usnic Acid Promotes Proteasomal and Autophagic Degradation of 14-3-3

Next, we examined the effect of UA on the protein levels. UA treatment decreased pan-14-3-3 protein levels in a time-dependent manner ([Figure 1D](#) and [Supplementary Figure S2A](#)). We used antibodies against the isoforms 14-3-3- ϵ and 14-3-3- σ . The upregulation of the 14-3-3- σ isoform differed from that of pan-14-3-3 blot ([Supplementary Figure S2B](#)).

The effect of UA treatment was investigated in the presence of proteasomal and lysosomal degradation inhibitors to determine whether the effect of UA on 14-3-3 proteins is mediated by autophagic or proteasomal pathways. As shown in [Figure 1E](#), cells were pretreated with the proteasome inhibitor MG132 (10 μ M), the lysosomal inhibitors bafilomycin A1 (100 nM) and chloroquine (CQ) (10 μ M), or the autophagosome blocker 3-MA (10 μ M) and, after that, treated with 10 μ M UA. Treatment with inhibitors reversed the degradation of 14-3-3 induced by UA, suggesting that UA downregulates 14-3-3 proteins through both proteasomal and autophagic pathways. To determine whether cell motility is associated with the degradation of 14-3-3, we performed cell invasion assays ([Figure 1F](#)). The results showed that UA decreased the invasion of CaCo2 cells, and this effect was restored by treatment with MG132, A1, CQ, and 3-MA. For further investigation, we performed qRT-PCR analysis in a time-dependent manner after 10 μ M treatment of usnic acid ([Supplementary Figure S3A–D](#)). The 14-3-3- β isoform's mRNA expression did not alter statistically significantly in the first 24 h when compared to DMSO, but after 48 h of therapy, its expression was 44% decreased. While UA may have induced mRNA-level compensatory 14-3-3- ϵ and 14-3-3- σ mRNA expression due to the decrease in protein level at 6th and 12th hours, the mRNA expression of 14-3-3- ϵ significantly regressed at 24th and 48th hours by treatment. UA marginally increased the mRNA expression of the 14-3-3- θ isoform. The expression of 14-3-3- γ , 14-3-3- η , and 14-3-3- ζ isoform mRNA tended to downregulate mRNA levels in a time-dependent nonspecific

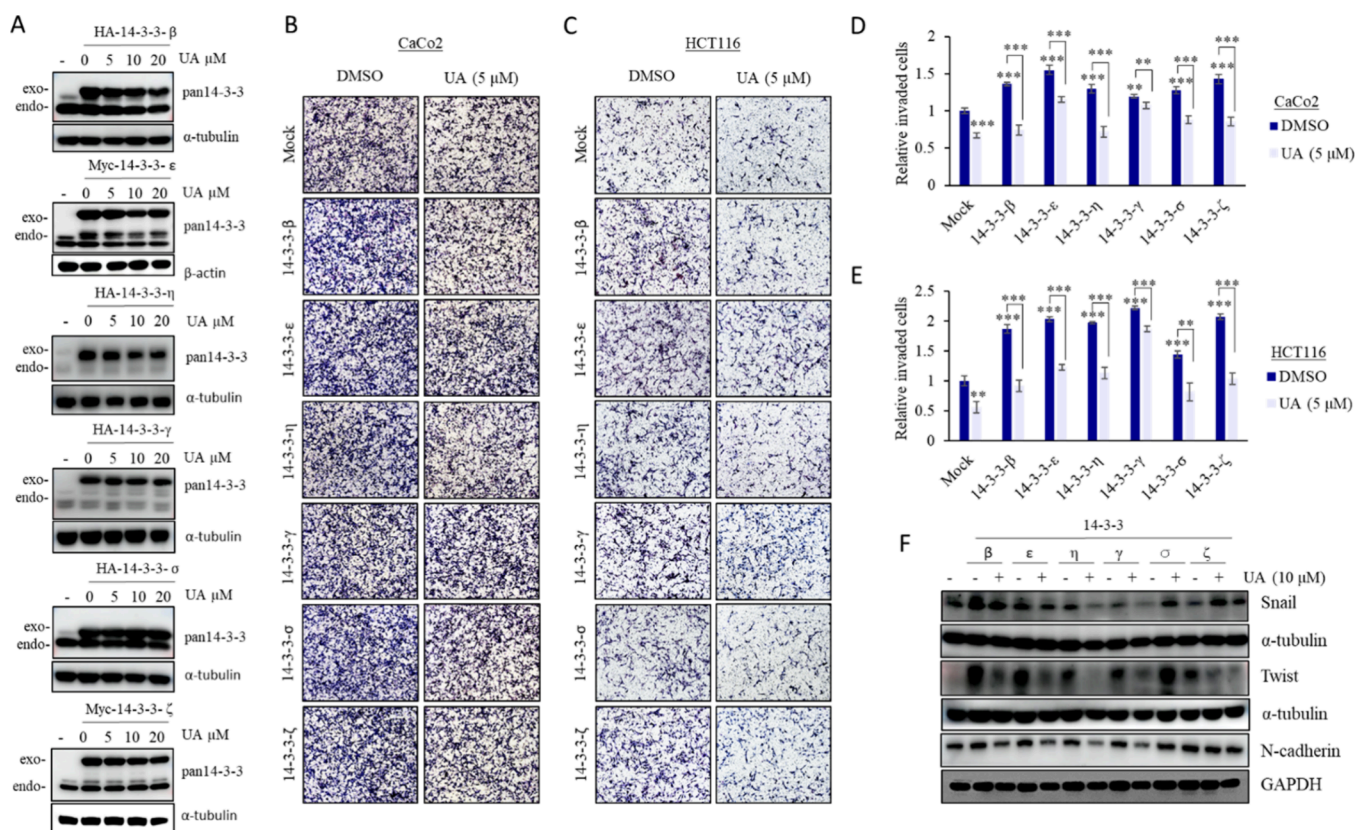


Figure 2. Effect of UA on the motility of cells overexpressing 14-3-3 isoforms. (A) CaCo2 cells were transfected with 14-3-3- β , 14-3-3- ϵ , 14-3-3- η , 14-3-3- σ , 14-3-3- γ , and 14-3-3- ζ plasmids for 24 h and treated with 5, 10, and 20 μ M UA for 48 h. 14-3-3 protein levels were assessed by western blotting. α -Tubulin or β -actin was used as a loading control. (B–E) CaCo2 and HCT116 cells were transfected with 14-3-3- β , 14-3-3- ϵ , 14-3-3- η , 14-3-3- σ , 14-3-3- γ , and 14-3-3- ζ isoforms for 24 h. Transfected cells were harvested and subjected to invasion assays. CaCo2 and HCT116 cells were treated with 5 μ M UA. (F) HCT116 cells were transfected with 14-3-3- β , 14-3-3- ϵ , 14-3-3- η , 14-3-3- σ , 14-3-3- γ , and 14-3-3- ζ isoforms for 24 h and then treated with 10 μ M UA for 24 h. Snail, Twist, and N-cadherin protein levels were assessed by western blotting. Data are presented as the mean \pm standard deviation. * p < 0.05; ** p < 0.01; *** p < 0.001.

manner. These results suggest that usnic acid interacts directly with 14-3-3 independently of mRNA activity.

Usnic Acid Suppresses Cell Invasion and Cell Cycle Progression in Cells Overexpressing 14-3-3 Isoforms

First, we examined the effect of UA on cells transfected with 14-3-3 isoforms using overexpression plasmids. UA downregulated overexpressed 14-3-3- β , 14-3-3- ϵ , 14-3-3- η , and 14-3-3- ζ protein levels, whereas it had no effect on overexpressed 14-3-3- σ and 14-3-3- γ protein levels (Figure 2A). Quantitative analysis of immunoblotting is given in Supplementary Figure S4. Next, we examined the effect of UA on cell invasiveness induced by the overexpression of 14-3-3 isoforms. UA treatment suppressed cell invasion induced by 14-3-3- β , 14-3-3- ϵ , 14-3-3- η , 14-3-3- σ , 14-3-3- γ , and 14-3-3- ζ overexpression in CaCo2 and HCT116 cells (Figure 2B–E). UA had the strongest inhibitory effect on cells transfected with 14-3-3- β and 14-3-3- ζ in both cell lines, whereas the effect of UA was weaker in cells transfected with 14-3-3- γ . Assessment of the effect of UA on the expression of epithelial-mesenchymal transition (EMT) markers upregulated by 14-3-3 overexpression showed that UA downregulated Snail, Twist, and N-cadherin protein levels (Figure 2F and Supplementary Figure S8A).

The 14-3-3 proteins serve as a critical integration site for many protein kinases and phosphatases that regulate the change from the G2 to M phase. We examined the effect of UA on the cell cycle by treating with UA at a concentration of 20 μ M in

overexpressed 14-3-3 isoform cells. UA decreased the population of cells in the G2/M phase and increased the G1 population. The inhibition in the G2/M phase population level was regressed compared with that in the mock control group in CaCo2 cells. HCT116 cells transfected with 14-3-3- ϵ , 14-3-3- η , 14-3-3- γ , and 14-3-3- σ showed a milder reduction of the G2/M phase than those transfected with the 14-3-3- β and 14-3-3- ζ isoforms (Supplementary Figures S5–S7).

Usnic Acid Regulates the Function of the 14-3-3 Protein and Inhibits the Client Protein Interaction/Phosphorylation

14-3-3 binds to Ser/Thr kinase proteins, thereby regulating their function. This was demonstrated in studies investigating mTOR, AMPK, MAPK, metabolism, apoptosis, and autophagy pathways through mediator proteins and phosphorylated proteins.^{21,59} To further characterize the inhibition of 14-3-3-mediated cell invasion, cell cycle progression, and metabolic activities by UA, we examined the levels of total and phosphorylated mTOR, Akt, JNK, STAT3, and NF- κ B, cell cycle checkpoint markers (cyclin B1, p-CDC2, and cyclin D1), autophagy markers (LCB3 and p62), and transcriptional regulator of β -catenin protein levels in cells transfected with 14-3-3 isoforms and treated with UA (Figure 3A–D). The results of quantitative analysis of immunoblotting data are shown in Supplementary Figure S9.

The sigma isoform of 14-3-3 plays a different role as a tumor suppressor,⁶⁰ although these findings are controversial. The

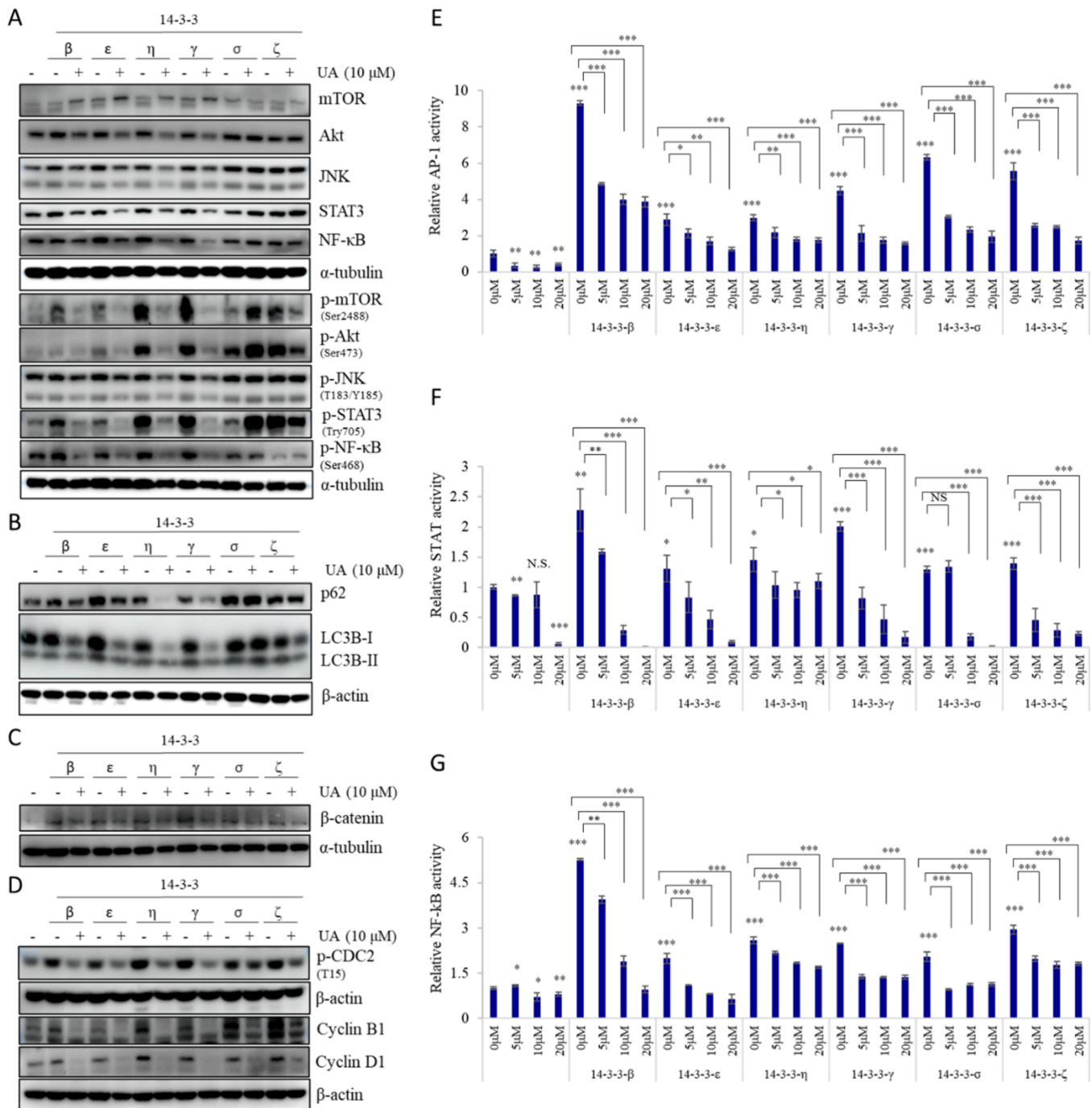


Figure 3. UA binds to 14-3-3 proteins and regulates target protein phosphorylation, autophagic markers, and transcriptional regulators. HCT116 cells were transfected with 14-3-3- β , 14-3-3- ϵ , 14-3-3- η , 14-3-3- σ , 14-3-3- γ , and 14-3-3- ζ isoforms for 24 h and then treated with 10 μ M UA for 24 h. Protein levels were assessed by western blotting. (A) Levels of mTOR, p-mTOR, Akt, p-Akt, JNK, p-JNK, p-STAT3, STAT3, p-NF- κ B, and NF- κ B. (B) Levels of p62 and LC3B. (C) Level of β -catenin. (D) Levels of p-CDC2, cyclin B1, and cyclin D1. GAPDH, α -tubulin, or β -actin was used as a loading control. UA suppressed the reporter activity of AP-1, NF- κ B, and STAT3 induced by 14-3-3 isoforms. 14-3-3- β , 14-3-3- ϵ , 14-3-3- η , 14-3-3- σ , 14-3-3- γ , and 14-3-3- ζ isoforms were cotransfected with (E) AP-1, (F) STAT, and (G) NF- κ B luciferase reporter plasmids in HEK293T cells for 24 h. Cells were treated with the indicated concentrations of UA for 48 h. Luciferase activity was determined using a Dual-Luciferase reporter assay system and normalized against Renilla luciferase activity. Data are presented as the mean \pm standard deviation. * p < 0.05; ** p < 0.01; *** p < 0.001; NS, no significant difference between compared groups.

present results showed that 14-3-3- σ is regulated positively and negatively depending on the interacting protein.

The involvement of 14-3-3 proteins in the regulation of the NF- κ B and STAT3 signaling pathways has been reported associated.⁶¹ The association of 14-3-3 with the upregulation of proteins such as MAPK and JNK targeting AP-1 has also been

reported.⁶² Therefore, we examined the effect of cotransfection with 14-3-3 isoforms and AP-1, STAT3, and NF- κ B luciferase plasmids in HEK293T cells. The results showed that transfection with 14-3-3- β , 14-3-3- ϵ , 14-3-3- η , 14-3-3- σ , 14-3-3- γ , and 14-3-3- ζ significantly increased AP-1, STAT3, and NF- κ B promoter activities. Treatment with UA at 5, 10, and 20 μ M

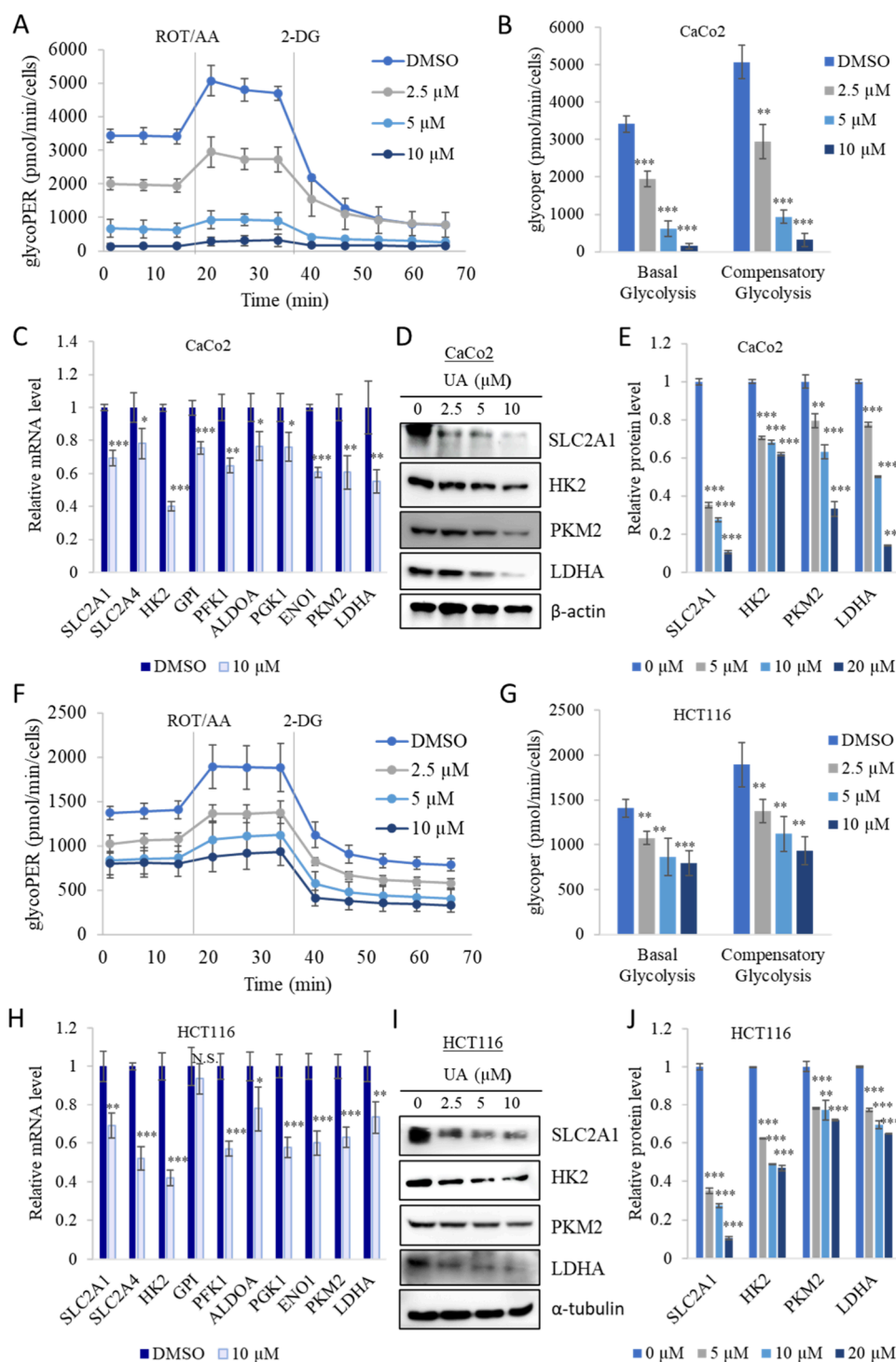


Figure 4. UA inhibits aerobic glycolysis in CRC cells. CaCo2 and HCT116 cells were treated with the indicated concentrations of UA (2.5, 5, or 10 μ M) for 48 h. (A, B, F, G) The Seahorse XF96 extracellular flux analyzer and Glycolytic Rate Assay Kit were used to measure the oxygen consumption rate (OCR) and extracellular acidification rate (ECAR). The assay uses both ECAR and OCR measurements to quantify glycolytic rates and calculate the glycolytic proton outflow rate (glycoPER). Following the sequential injection of rotenone/antimycin A and 2-DG, measurements were obtained at two time points. The glycolysis rate assay provides the basal glycolysis and compensatory glycolysis parameters. Data are presented as the mean \pm standard deviation, $n = 3$. * $p < 0.05$; ** $p < 0.01$; *** $p < 0.001$; NS, not significant vs the DMSO-treated group. (C, H) Potential UA targets were identified by qRT-PCR to explore the effects of UA on aerobic glycolysis. The mRNA levels of SLC2A1, SLC2A4, HK2, GPI, PFK1, ALDOA, PGK1, ENO1, PKM2, and LDHA were determined in CRC cells treated with 10 μ M UA for 48 h. Data are presented as the mean \pm standard deviation, $n = 3$. * $p < 0.05$; ** $p < 0.01$; *** $p < 0.001$; NS, not significant vs the DMSO-treated group. (D, E) CaCo2 and (I, J) HCT116 cells were treated with 10 μ M UA, and SLC2A1, HK2, PKM2, and LDHA protein levels were detected by western blotting. α -Tubulin or β -actin was used as a loading control. Values are presented as arbitrary units of densitometry corresponding to signal intensity. * $p < 0.05$; ** $p < 0.01$; *** $p < 0.001$; NS, not significant vs the DMSO-treated group.

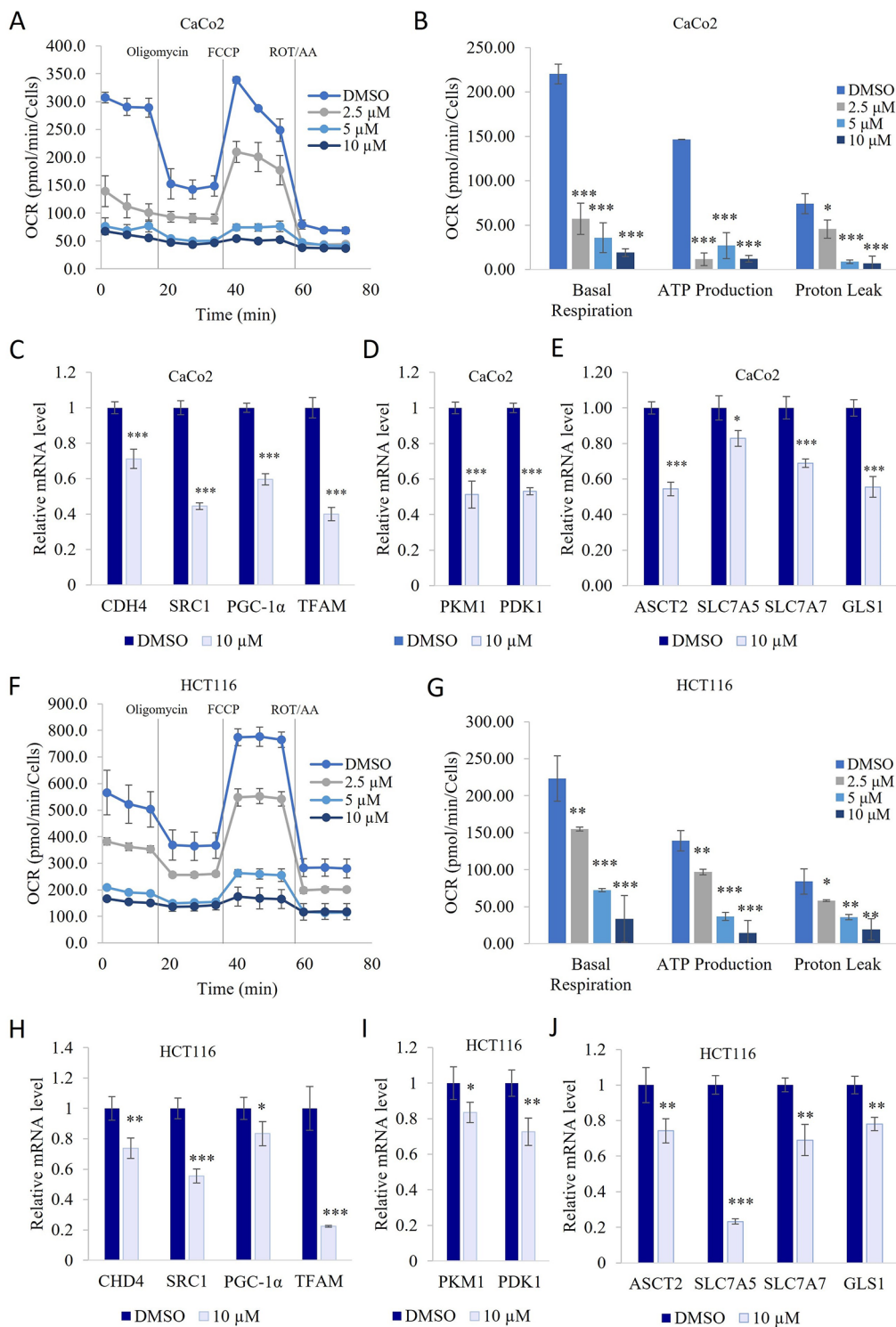


Figure 5. UA suppresses mitochondrial respiration and glutaminolysis in CRC cells. (A, B) CaCo2 and (F, G) HCT116 cells were treated with the indicated concentrations of UA (2.5, 5, and 10 μ M) for 48 h. The Cell Mito Stress Test Kit and Seahorse XF96 extracellular flux analyzer were used to determine the oxygen consumption rate (OCR). To test basal respiration, proton leakage, and ATP generation, the OCR was measured after oligomycin, FCCP, rotenone/antimycin A sequential injection. Data are presented as the mean \pm standard deviation, $n = 3$. * $p < 0.05$; ** $p < 0.01$; *** $p < 0.001$. To clarify the mechanisms by which UA modulates mitochondrial respiration and glutaminolysis, we performed qRT-PCR to detect possible target genes of UA. The mRNA levels of CDH4, SRC1, PGC-1 α , TFAM, PKM1, PDK1, ASCT2, SLC7A5, SLC7A7, and GLS1 were measured in CRC cells treated with 10 μ M UA for 48 h. (C–E) CaCo2 and (H–J) HCT116 cells. Data are presented as the mean \pm standard deviation. * $p < 0.05$; ** $p < 0.01$; *** $p < 0.001$.

significantly decreased the activity of AP-1, STAT3, and NF- κ B induced by 14-3-3 isoform plasmids (14-3-3- σ -induced STAT3 activity, except in the presence of 5 μ M UA). These results

indicate that 14-3-3 isoforms regulate AP-1, STAT3, and NF- κ B signaling, and UA treatment targeting 14-3-3 suppresses their activity (Figure 3E–G).

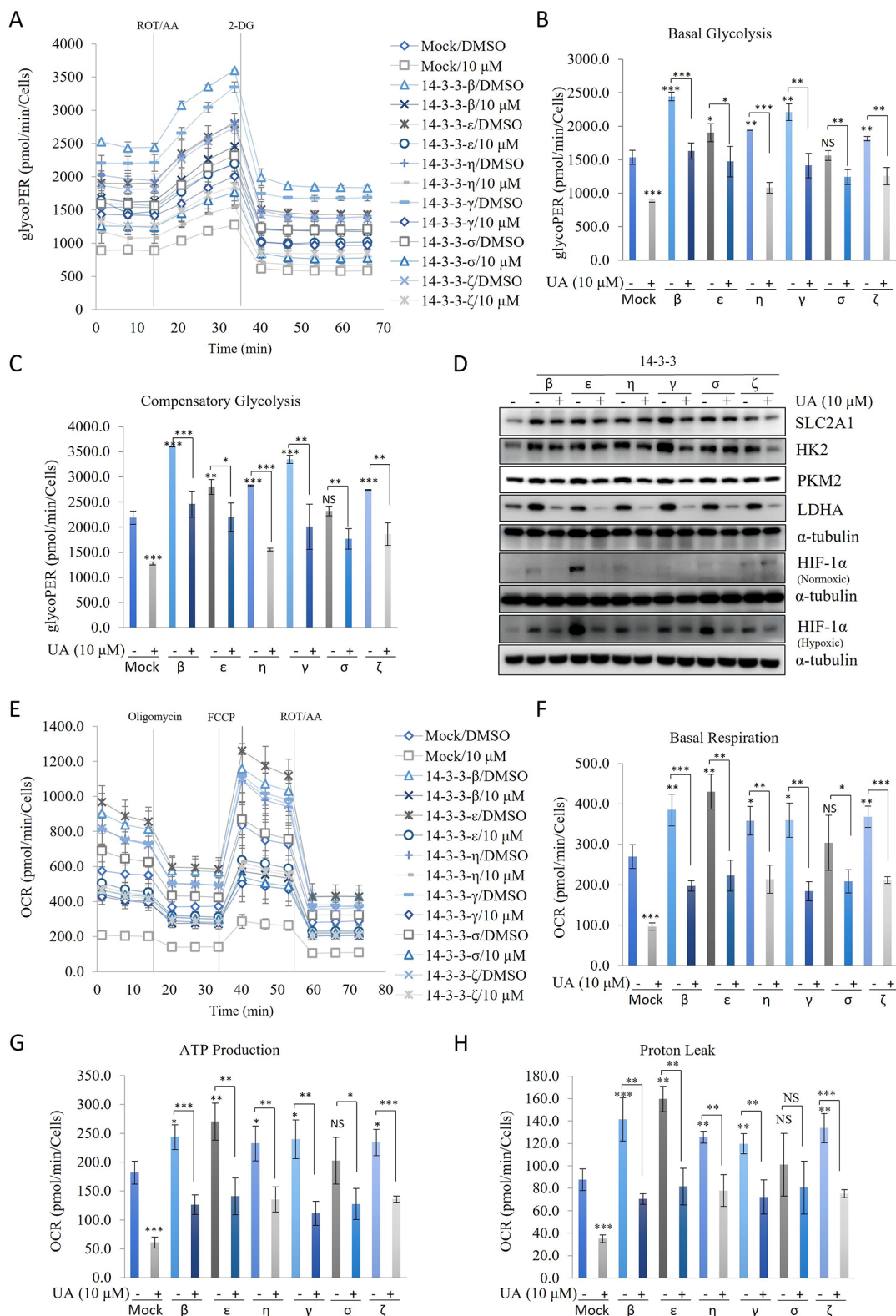


Figure 6. UA regulates cell metabolism via 14-3-3 proteins. CaCo2 cells were transfected with the 14-3-3- β , 14-3-3- ϵ , 14-3-3- η , 14-3-3- σ , 14-3-3- γ , and 14-3-3- ζ isoforms for 24 h, harvested, and then subjected to glycoPER and OCR measurements for 48 h. (A–C) UA suppressed the glycolysis rate, basal glycolysis, and compensatory glycolysis in CaCo2 cells induced with 14-3-3 isoforms. (D) HCT116 cells were transfected with the 14-3-3- β , 14-3-3- ϵ , 14-3-3- η , 14-3-3- σ , 14-3-3- γ , and 14-3-3- ζ isoforms for 24 h and then treated with 10 μ M UA for 24 h. SLC2A1, HK2, PKM2, LDHA, and HIF1- α (hypoxic and normoxic) protein levels were assessed by western blotting. (E–H) UA decreased OCR, basal respiration, ATP production, and proton leakage. Data are presented as the mean \pm standard deviation. * p < 0.05; ** p < 0.01; *** p < 0.001; NS, not significant vs DMSO-treated or mock-transfection groups.

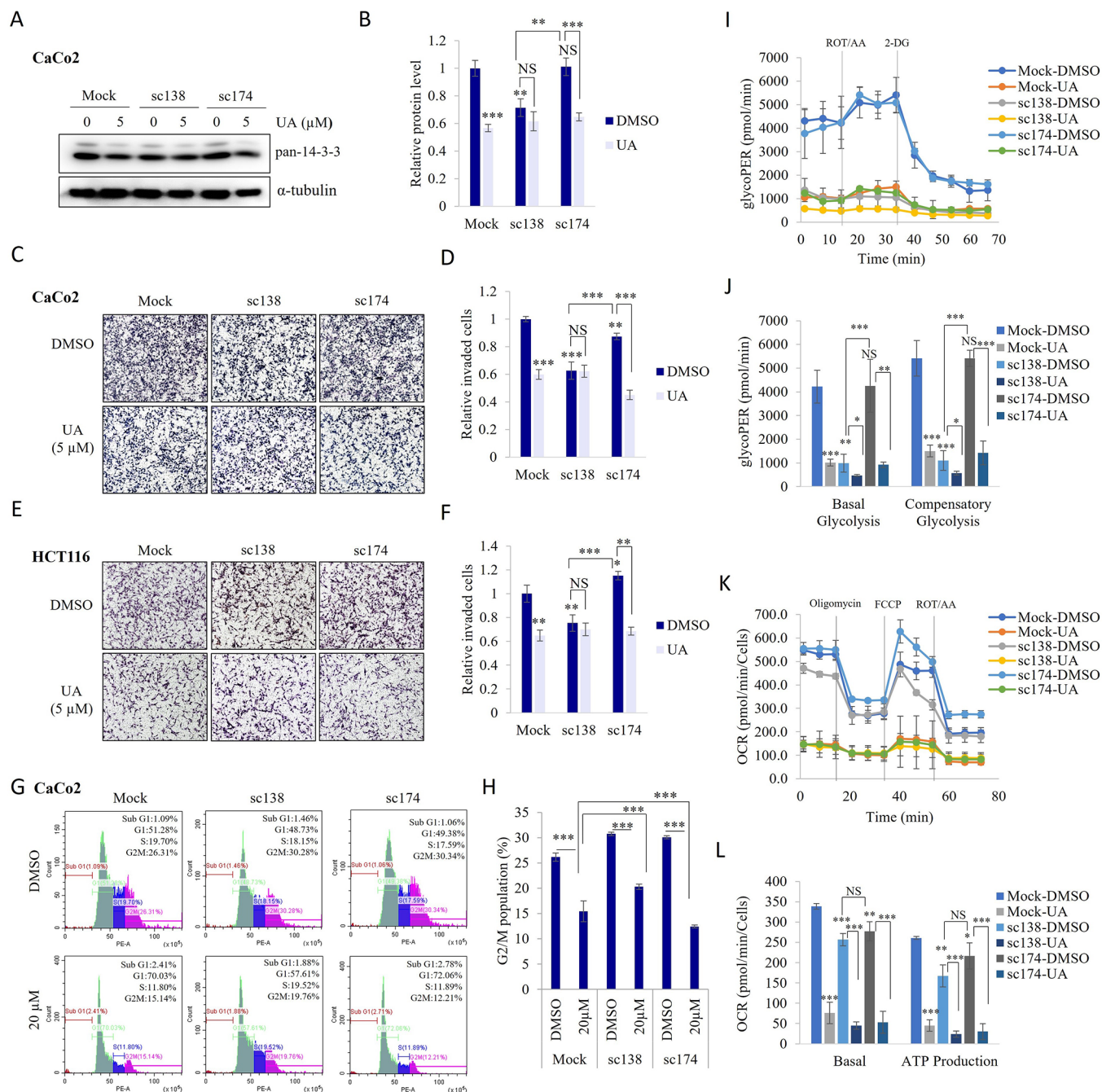


Figure 7. sc138, a specific peptide inhibitor of 14-3-3 substrate interactions, weakens or blocks the effect of UA. (A, B) Pan-14-3-3 protein levels were assessed in CaCo2 cells transfected with sc138 or sc174 and treated with UA at 24 h post-transfection. α -Tubulin was used as a loading control. Values are presented as arbitrary units of densitometry corresponding to signal intensity. (C–F) CaCo2 and HCT116 cells were transfected with sc138 or the nonfunctional mutant inhibitor sc174 for 24 h, harvested, and subjected to invasion assays. Cells treated with 5 μ M UA. Data are presented as the mean \pm standard deviation; $n = 3$. * $p < 0.05$; ** $p < 0.01$; *** $p < 0.001$; NS, no significant difference compared with each group. (G, H) Flow cytometric analysis of cell cycle distribution. CaCo2 cells were transfected with sc138 and sc174 and treated with 20 μ M UA. Data are presented as the mean \pm standard deviation; $n = 3$. * $p < 0.05$; ** $p < 0.01$; *** $p < 0.001$. (I–L) CaCo2 cells were transfected with sc138 and sc174 for 24 h. Cells were harvested and subjected to glycoPER or OCR measurement after treatment with 10 μ M UA for 48 h. Data are presented as the mean \pm standard deviation, $n = 3$. * $p < 0.05$; ** $p < 0.01$; *** $p < 0.001$; NS, no significant difference vs the DMSO-treated group.

Usnic Acid Suppresses Aerobic Glycolysis, Mitochondrial Biogenesis, and Glutaminolysis and Decreases the 14-3-3-Mediated Glycolytic Proton Outflow Rate (glycoPER) and Oxygen Consumption Rate (OCR)

We tested the glycolytic function in CaCo2 and HCT116 cells based on the extracellular acidification rate (ECAR) determined by the glycolytic rate assay using an antimycin/rotenone and

2-deoxy-D-glucose (2-DG) (Figure 4A,F). UA significantly decreased basal glycolysis and compensatory glycolysis, glycolytic rate assay parameters in both cell lines (Figure 4B,G). We then checked the mRNA levels of enzymes involved in the aerobic glycolysis pathway (SLC2A1, SLC2A4, HK2, GPI, PFK1, ALDOA, PGK1, ENO1, PKM2, and LDHA). UA at 10 μ M downregulated the mRNA expression of these markers in

CaCo2 and HCT116 cells (Figure 4C,H). The protein levels of SLC2A1, HK2, PKM2, and LDHA were downregulated by UA in a dose-dependent manner, whereas the mRNA expression was downregulated in both cell lines (Figure 4D,E,I,J).

To examine the effect of UA on mitochondrial biogenesis in CRC, the OCR was assessed by using a Seahorse XFe96 analyzer. OCR analysis allows real-time monitoring of mitochondrial respiration by assessing parameters such as ATP production, basal respiration, and proton leakage after oligomycin, FCCP, and antimycin/rotenone mix treatment, respectively.¹³ UA significantly decreased mitochondrial respiration in CaCo2 and HCT116 cells by suppressing basal respiration, ATP production, and proton leakage (Figure 5A,B,F,G).

Next, we examined the mRNA expression of relevant markers to elucidate the mechanisms underlying the effect of UA on inhibiting the mitochondrial biogenesis pathway in CaCo2 and HCT116 cells. UA downregulated the expression of the mitochondrial transcription factor TFAM⁶³ and key markers of mitochondrial processes (CHD4, PGC1- α , and SRC-1) necessary for mitochondrial respiration (Figure 5C,H). Treatment with UA (10 μ M) downregulated pyruvate kinase M (PKM)-1 and pyruvate dehydrogenase kinase (PDK)-1 mRNA (Figure 5D,I). PKM1 is an isoform of PKM, and its expression is associated with oxidative phosphorylation.⁶⁴ PDK1 inhibits the use of pyruvate in the TCA cycle by preventing its conversion to acetyl CoA.⁶⁵ Similarly, UA downregulated the expression of target genes involved in glutaminolysis such as ASCT2, SLC7A5, SLC7A7, and GLS1 (Figure 5E,J).

To demonstrate that UA modulates 14-3-3-mediated metabolic activities, we controlled for glycolytic rate and the OCR levels induced by isoforms of 14-3-3. Except for the 14-3-3- σ isoform, the remaining isoforms 14-3-3- β , 14-3-3- ϵ , 14-3-3- η , 14-3-3- γ , and 14-3-3- ζ significantly upregulated basal glycolysis, compensatory glycolysis, basal respiration, ATP production, and proton leakage. The GLUT1, HK2, PKM2, and LDHA markers induced by 14-3-3 isoforms and the protein levels of HIF-1 α (under normoxic and hypoxic conditions), which are involved in metabolic regulation, were examined after treatment with DMSO or UA. UA significantly suppressed 14-3-3-induced glycolysis and mitochondrial respiration (Figure 6A–H and Supplementary Figure S8B,C).

A Peptide Inhibitor of 14-3-3 Blocks/Regresses Usnic Acid Activity

Most activity of usnic acid is blocked/regressed in cells transfected with sc138 (a 14-3-3 peptide inhibitor) such as suppressing cell invasion, cell cycle, glycoPER, OCR, and luciferase activity of AP-1, STAT, and NF- κ B. The protein level of 14-3-3 was assessed in cells transfected with mock, sc138, and sc174 constructs. Figure 7A–F shows that sc138 blocked the inhibition of 14-3-3 protein levels by UA treatment and suppressed the effect of UA on decreasing the cell invasion in CaCo2 and HCT116 cells. By contrast, a nonfunctional mutant inhibitor of sc174 transfection did not affect UA activity. Next, we performed flow cytometry analysis of the cell cycle. Transfection with sc138 attenuated the UA-induced reduction in the G2/M population compared with cells transfected with mock and sc174, although it did not completely block the effect of UA on the cell cycle (Figure 7G,H and Supplementary Figure S10). This suggests that sc138 transfection does not completely block the interactions of 14-3-3 with cell cycle-related proteins. Next, we investigated the effects of cotransfection of sc138 with

AP-1, STAT3, or NF- κ B luciferase plasmids. The 14-3-3 peptide inhibitor sc138 downregulated AP-1, STAT3, and NF- κ B activities and regressed the activity of UA (Supplementary Figure S11). Finally, we investigated the effect of UA treatment on glycoPER and OCR in the presence of sc138. Usnic acid showed an inhibition of approximately 75% and more when compared with DMSO in mock transfection, while sc138 could inhibit glycolysis by approximately 50% compared to the DMSO group in transfected cells. In sc138-transfected CaCo2 cells, glycoPER basal and compensatory parameters were suppressed, and sc138 regressed the inhibitory effect of UA compared with the control groups (Figure 7I,J). Transfection with sc138 decreased the level of the oxygen consumption rate (OCR) in CaCo2 cells, although it did not proportionally decrease the inhibitory effect of UA (Figure 7K,L). In the HCT116 cell line, sc138 transfection significantly decreased the inhibitory effect of UA compared with that in other groups (Supplementary Figure S12). Overall, the present results provide evidence that 14-3-3 proteins regulate the activity of UA, as indicated by the effect of 14-3-3 on suppressing the activity of UA after transfection with a peptide inhibitor.

DISCUSSION

The expression of 14-3-3 proteins in CRC tissues has been reported in clinical and experimental studies. The 14-3-3 proteins are located in the cytosol or nucleus or in close proximity to the plasma membrane.⁶⁶ The aminoterminal α helix domain of 14-3-3 proteins enables them to interact with a wide range of signaling proteins, kinases (Ser/Thr kinase), cytoskeletal proteins, metabolic enzymes, phosphatases, and transcription factors.^{67,68} In cancer patients, overexpression of 14-3-3 proteins is associated with drug resistance, poor prognosis, and low survival, suggesting that the 14-3-3 proteins are potential targets for the treatment of cancer.⁶⁹

Here, we examined the processes modulated by the 14-3-3 protein and explored the effect of UA, a molecule of lichen origin that binds to 14-3-3, on these processes. UA bound to and downregulated 14-3-3 proteins at different time points, and the decrease in protein levels after 6 h of treatment suggested that UA interacts directly with the 14-3-3 protein. This impaired the function of 14-3-3 and its oncogenic role and induced proteasomal and autophagic degradation. We then used sc138, a 14-3-3 peptide inhibitor, to block the activity of UA and assessed cell invasion, cell cycle progression, glycoPER, luciferase reporter activity (NF- κ B, STAT3, and AP-1), and 14-3-3 protein levels. The results showed that the activity of UA was suppressed by the 14-3-3 peptide inhibitor and indicated that its anticancer activity was mediated by 14-3-3. However, although it attenuated the activity of UA on the cell cycle, the changes were not statistically significant, suggesting that sc138 failed to block all kinase domains. UA downregulated protein levels of 14-3-3 in cells overexpressing the 14-3-3- β , 14-3-3- ϵ , 14-3-3- η , and 14-3-3- ζ isoforms, whereas it had no reduction effect on the levels of the 14-3-3- γ and 14-3-3- σ isoforms. Isoforms may contribute differently to tumor formation in different types of cancer. 14-3-3- σ has been reported to be expressed at low levels in lung, breast, esophageal, chronic myeloid leukemia, uterine, ovarian, and skin cancer. 14-3-3- σ is overexpressed in ductal cancers of the liver and pancreas. 14-3-3- γ is reported to be overexpressed in liver, prostate, and lung cancer. While 14-3-3- ζ and 14-3-3- β are associated with colon cancer, 14-3-3- ϵ is associated with gastric cancer.⁷⁰ The reported specificity of 14-3-3 isoforms to different types of cancer and

their varying potential in tumor formation suggest that the therapeutic effects of UA may vary.

The 14-3-3 peptide inhibitor blocked the effect of UA on cell motility. We tested the cell motility activity of UA in cells transfected with 14-3-3 isoforms, and the results showed that UA dramatically inhibited cell motility in the 14-3-3- β and 14-3-3- ζ isoform-transfected cells compared to the control and other isoforms. UA inhibits cell motility in lung, colorectal, and prostate cancers and in melanoma,^{71–73} and EMT markers are used to characterize the effect of UA on cell motility.¹² EMT is a crucial regulator of metastasis because it facilitates the invasion and spread of tumor cells to distant tissues.⁷⁴ The association of 14-3-3 isoforms with EMT markers was reported previously.^{75–78} Therefore, we measured the levels of N-cadherin, Twist, and Snail induced by the 14-3-3 isoforms. In cells transfected with the 14-3-3- σ and 14-3-3- ζ isoforms, N-cadherin levels were not downregulated, whereas UA downregulated the other markers in all isoform-induced cells.

Studies show that UA increases the population of cells in the G1 phase.⁷⁹ Cell cycle checkpoints are controlled by p-CDC2 (T15), cyclin D1, and cyclin B1. 14-3-3 proteins play a role in cancer development and progression by affecting cell cycle progression. Different 14-3-3 isoforms deregulate the cell cycle by affecting the phosphorylation or kinase partners of CDK2/4, CDC25A, CDC25B, p27, FOXO1, MIZ1, and p53.⁸⁰ In this study, treatment with 20 μ M UA increased the G1 phase population, and exposure to 10 μ M UA downregulated the checkpoint markers p-CDC2 (T15), cyclin D1, and cyclin B1 in cells overexpressing 14-3-3 isoforms. Taken together, the results of the cell cycle analysis suggest that UA promotes the G1 phase of the cycle by modulating 14-3-3 proteins.

14-3-3 proteins interact with target proteins and regulate the phosphorylation of several proteins. Studies show that 14-3-3 controls Akt during intestinal inflammation and that inhibition of 14-3-3 interactions with BVO2 regulates Akt activity and triggers the death of intestinal epithelial cells.⁸¹ In addition, JNK activates the 14-3-3 protein and antagonizes Akt-mediated Beclin-1 phosphorylation to regulate autophagy.⁸² JNK controls the phosphorylation of 14-3-3 to promote Bax activation.⁸³ 14-3-3 proteins play a regulatory role in cellular processes that trigger autophagy by interacting with proteins such as mTOR, MAPK, and PI3K.⁸⁴ 14-3-3 proteins bind to TSC2 and PRAS40, which act as mTOR regulators, thereby playing a role in mTOR-regulated cellular processes.^{85,86} UA induces autophagy and apoptosis by inhibiting the AKT, mTOR, ERK1/2, and JNK signaling pathways.^{87,88} Important regulators of the autophagic process include P62 and LC3B-I/II. Conversion of LC3B-I to LC3B-II and binding of LC3B to p62 facilitate autophagic degradation.⁵⁸ Current results indicate that the activity of UA involves the regulation of 14-3-3 proteins, which is consistent with previous reports of the effect of UA on signaling pathways related to cell death.

Numerous illnesses, including cancer, diabetes, obesity, and cardiovascular disease, have metabolic pathway-related disorders, which are linked to the wide distribution of potential 14-3-3 targets.²¹ To the best of our knowledge, this is the first study investigating the effect of UA on glycolysis, metabolic biogenesis, and glutaminolysis. Cancer cell proliferation, resistance to therapies, and metastasis are related to the reorganization of metabolic pathways. Metabolic pathways such as glycolysis, mitochondrial respiration, glutaminolysis, and lipid metabolism play a role in energy production in cancer.⁶⁰ Cancer cells activate aerobic glycolysis in the presence

of oxygen for bioenergetic processes. These processes are mediated by a number of catalytic enzymes and promote the production of pyruvate to lactate.¹³ We showed that UA downregulates several aerobic glycolysis markers, including GLUTs, HKs, PKM2, and LDHA. The kinase activity of PKM2 involves interaction with 14-3-3 proteins via the binding of 14-3-3 to Akt.⁸⁹ 14-3-3- ζ is responsible for LDHA expression and plays a role in the initiation and progression of breast cancer.⁹⁰ Mitochondrial respiration, the main source of cellular energy production, is associated with the downregulation of TFAM, CDH4, SRC1, PGC-1 α , PKM1, and PDK1, which act as key markers in mitochondrial processes. UA treatment downregulates key markers of mitochondrial processes. 14-3-3 binds to phosphorylated PDK1, thereby displacing PDK1 from the cytoplasmic membrane,⁹¹ and UA downregulates phosphorylated PDK1.⁸⁸ Similarly, UA downregulates the expression of ASCT2, SLC7A5, SLC7A7, and GLS1, which are involved in glutaminolysis. Here, we showed the effect of UA on inhibiting 14-3-3-mediated aerobic glycolysis and mitochondrial biogenesis.

Metabolic signaling pathways, cell cycle progression, and cell motility are modulated by transcriptional regulators and transcriptional cofactors. To further characterize the activity of UA mediated by 14-3-3 proteins, we assessed the levels of transcriptional regulators such as AP-1, β -catenin, HIF-1 α , NF- κ B, and STAT3 in the presence of 14-3-3 isoforms. The AP-1 transcription factor plays a role in cancer-related processes including cell invasion, metastasis, cell proliferation, immune responses, and cell metabolism in different types of cancer.^{92,93} Upregulation of 14-3-3 proteins results in AP-1 activation.^{94,95} In this study, AP-1 activity was induced by six 14-3-3 isoforms, and UA treatment suppressed this effect. β -Catenin, the target of the WNT signaling pathway, is an oncogene that acts as a transcriptional regulator.⁹⁶ β -Catenin and 14-3-3 form “bleb-like” structures, and the interaction of 14-3-3- ζ with β -catenin plays a role in cell motility and oncogenic signaling.⁹⁷ We found that β -catenin was induced by 14-3-3 isoforms and UA suppressed this effect. In a previous study, UA suppressed AP-1 and β -catenin-mediated TOPFLASH reporter activity and the downstream target genes of β -catenin/LEF and c-jun/AP-1.¹⁴ Another transcription factor, HIF-1 α , plays a role in regulating angiogenesis, metastasis, cell survival, invasion, and metabolic pathways in cancer. PKM2 acts as a coactivator of HIF-1 α and regulates the expression of genes encoding GLUT1, LDHA, and PDK1.⁹⁸ We examined the levels of HIF-1 α in cells transfected with 14-3-3 isoforms under normoxic and hypoxic conditions and showed that UA downregulates HIF-1 α levels. NF- κ B and STAT3, two transcription factors associated with cancer and inflammation, play vital roles in cellular processes.⁹⁹ UA decreased STAT3 and NF- κ B reporter activity induced by 14-3-3 isoform overexpression. 14-3-3- ζ interacts with the JAK/STAT pathway or STAT3,^{100–102} and UA downregulates STAT3.¹⁰³

Here, we examined the anticancer activity of UA mediated by its target 14-3-3 and the effect of UA on the regulation of signaling pathways induced by 14-3-3 proteins. In addition, based on previous experimental and clinical studies, we examined the effects of different isoforms of 14-3-3, thereby providing a broad perspective of the effect of 14-3-3 on cancer-related processes such as the Akt/mTOR/JNK signaling pathways, EMT, metabolism, cell motility, cell cycle, autophagy, and transcriptional regulators. Increasing evidence supports the role of 14-3-3 in chemotherapy resistance and poor survival. The

14-3-3 isoforms β , γ , and σ are upregulated in 5-fluorouracil-resistant cells compared with DLD-1 parent cells.¹⁰⁴ UA shows therapeutic potential and can be used in combination with chemotherapeutics in the targeting 14-3-3 protein therapies. Consequently, we define UA as a molecule targeting 14-3-3.

CONCLUSIONS

We report that usnic acid, whose activities have been reported in many different cancer types for many years, binds to isoforms of 14-3-3 proteins, a master regulator protein, via a chemical probe. Usnic acid downregulates the levels of 14-3-3-mediated client/phosphorylated proteins, cell invasion, aerobic glycolysis, and oxidative phosphorylation. Collectively, our study sheds light on the elucidated mechanisms underlying the anticancer activity of usnic acid. Our findings suggest a new strategy to develop therapeutics against treatment resistance as well as higher expression of 14-3-3 proteins in colorectal cancer or in multiple cancer progressions.

ASSOCIATED CONTENT

Data Availability Statement

The data sets supporting conclusions of this article are available from the corresponding author upon reasonable request.

Supporting Information

The Supporting Information is available free of charge at <https://pubs.acs.org/doi/10.1021/jacsau.3c00774>.

GEPIA database data, protein levels, mRNA expressions, cell cycle, reporter assay, oxygen consumption rate, confocal images, primer sequences for qRT-PCR, and antibody and plasmid information (PDF)

AUTHOR INFORMATION

Corresponding Author

Hangun Kim – College of Pharmacy, Suncheon National University, Jeonnam 57922, Republic of Korea; orcid.org/0000-0001-5889-8907; Phone: +82-61-750-3761; Email: hangunkim@sunchon.ac.kr

Authors

Mücahit Varlı – College of Pharmacy, Suncheon National University, Jeonnam 57922, Republic of Korea
Suresh R. Bhosle – College of Pharmacy, Suncheon National University, Jeonnam 57922, Republic of Korea
Eunae Kim – College of Pharmacy, Chosun University, Gwangju 61452, Republic of Korea; orcid.org/0000-0001-8538-7336
Yi Yang – College of Pharmacy, Suncheon National University, Jeonnam 57922, Republic of Korea
İsa Taş – College of Pharmacy, Suncheon National University, Jeonnam 57922, Republic of Korea
Rui Zhou – College of Pharmacy, Suncheon National University, Jeonnam 57922, Republic of Korea
Sultan Pulat – College of Pharmacy, Suncheon National University, Jeonnam 57922, Republic of Korea
Chathurika D. B. Gamage – College of Pharmacy, Suncheon National University, Jeonnam 57922, Republic of Korea
So-Yeon Park – College of Pharmacy, Suncheon National University, Jeonnam 57922, Republic of Korea
Hyung-Ho Ha – College of Pharmacy, Suncheon National University, Jeonnam 57922, Republic of Korea

Complete contact information is available at:

<https://pubs.acs.org/10.1021/jacsau.3c00774>

Author Contributions

M.V. and H.K. conceived and designed the study. M.V. performed most of the experiments. S.R.B. and H.-H.H. prepared the chemical probe for protein identification. E.K. provided critical review of the manuscript. Y.Y., İ.T., R.Z., S.P., C.D.B.G., and S.-Y.P. performed part of the experiments. M.V. and H.K. analyzed the data and wrote the manuscript. All authors have read and approved the final submitted manuscript. CRediT: **Mücahit Varlı** conceptualization, investigation, visualization, writing-original draft; **Suresh R. Bhosle** methodology, resources, validation; **Eunae Kim** methodology; **Yi Yang** investigation; **İsa Taş** investigation; **Rui Zhou** investigation; **Sultan Pulat** investigation; **Chathurika D. B. Gamage** investigation; **So-Yeon Park** investigation; **Hyung-Ho Ha** methodology, resources, validation; **Hangun Kim** conceptualization, project administration, writing-review & editing.

Funding

This work was supported by the National Research Foundation of Korea grant (RS-2023-00250803) funded by the Korea government (MSIP).

Notes

The authors declare no competing financial interest.

ACKNOWLEDGMENTS

The authors thank Dr. Kwonseop Kim from the College of Pharmacy and Research Institute of Drug Development, Chonnam National University for sc138 and sc174 plasmids. The authors thank Dr. Ick Young Kim from the Laboratory of Cellular and Molecular Biochemistry, School of Life Sciences and Biotechnology for the HA-14-3-3 η plasmid. The authors thank Dr. Kwang-Youl Lee from the College of Pharmacy and Research Institute of Drug Development, Chonnam National University for PCS4 + 3myc-14-3-3- ϵ , pcDNA3-HA-14-3-3- γ , pcDNA3-HA-14-3-3- β , Myc-14-3-3- ζ , and pcDNA3-HA-14-3-3- σ plasmids.

ABBREVIATIONS

AP-1: activator protein 1
ASCT2: alanine/serine/cysteine-preferring transporter 2
ALDOA: aldolase, fructose-bisphosphate A
BSA: bovine serum albumin
CRC: colorectal cancer
CHD4: chromodomain helicase DNA binding protein 4
COAD: colon cancer
DMSO: dimethyl sulfoxide
ECAR: extracellular acidification rate
EMT: epithelial-mesenchymal transition
ENO1: enolase 1
GLS1: glutaminase
GPI: glucose-6-phosphate isomerase
HK2: hexokinase 2
HIF-1 α : hypoxia-inducible factor 1-alpha
LDHA: lactate dehydrogenase A
MALDI-TOF MS: matrix-assisted laser desorption/ionization time-of-flight mass spectrometry
NF-KB: nuclear factor kappa-light-chain-enhancer of activated B
OCR: oxygen consumption rate
PDK1: pyruvate dehydrogenase kinase 1

PFK1: phosphofructokinase-1
 PGK1: phosphoglycerate Kinase 1
 PGC-1 α : peroxisome proliferator-activated receptor gamma coactivator 1 alpha
 PKM1: pyruvate kinase M1
 PKM2: pyruvate kinase M2
 SLC7A5: solute carrier family 7 member 5
 SLC7A7: solute carrier family 7 member 7
 SLC2A1: solute carrier family 2 member 1
 SLC2A4: solute carrier family 2 member 4
 TFAM: transcription factor A, mitochondrial
 UA: usnic acid

REFERENCES

- Xie, Y. H.; Chen, Y. X.; Fang, J. Y. Comprehensive Review of Targeted Therapy for Colorectal Cancer. *Signal Transduction and Targeted Therapy* 2020 5:1 **2020**, 5 (1), 1–30.
- Hawk, E. T.; Levin, B. Colorectal Cancer Prevention. *Journal of Clinical Oncology* **2005**, 23 (2), 378–391.
- Waldner, M. J.; Neurath, M. F. The Molecular Therapy of Colorectal Cancer. *Mol. Aspects Med.* **2010**, 31 (2), 171–178.
- Fakih, M. G. Metastatic Colorectal Cancer: Current State and Future Directions. *Journal of Clinical Oncology* **2015**, 33 (16), 1809–1824.
- Kumar, K.; Mishra, J. P. N.; Singh, R. P. Usnic Acid Induces Apoptosis in Human Gastric Cancer Cells through ROS Generation and DNA Damage and Causes Up-Regulation of DNA-PKcs and γ -H2A.X Phosphorylation. *Chem. Biol. Interact* **2020**, 315, No. 108898.
- TAS, I. S. A. Evaluation Of Pharmaceutical Potential And Phytochemical Analysis Of Selected Traditional Lichen Species. *Farmacja* **2021**, 69, 6.
- Tas, I.; Yildirim, A. B.; Ozkan, E.; Ozyigitoglu, G. C.; Yavuz, M. Z.; Turker, A. U. Biological Evaluation and Phytochemical Profiling of Some Lichen Species. *Acta Aliment* **2019**, 48 (4), 457–465.
- Geng, X.; Zhang, X.; Zhou, B.; Zhang, C.; Tu, J.; Chen, X.; Wang, J.; Gao, H.; Qin, G.; Pan, W. Usnic Acid Induces Cycle Arrest, Apoptosis, and Autophagy in Gastric Cancer Cells In Vitro and In Vivo. *Med. Sci. Monit* **2018**, 24, 556.
- Yoo, K. H.; Kim, D. H.; Oh, S.; Park, M. S.; Kim, H.; Ha, H. H.; Cho, S. H.; Chung, I. J.; Bae, W. K. Transcriptome Analysis upon Potassium Usnate Exposure Reveals ATF3-Induced Apoptosis in Human Gastric and Colon Cancer Cells. *Phytomedicine* **2021**, 91, No. 153655.
- Bačkorová, M.; Bačkor, M.; Mikeš, J.; Jendželovský, R.; Fedoročko, P. Variable Responses of Different Human Cancer Cells to the Lichen Compounds Parietin, Atranorin, Usnic Acid and Gyrophoric Acid. *Toxicology in Vitro* **2011**, 25 (1), 37–44.
- Lee, S.; Lee, Y.; Ha, S.; Chung, H. Y.; Kim, H.; Hur, J. S.; Lee, J. Anti-Inflammatory Effects of Usnic Acid in an MPTP-Induced Mouse Model of Parkinson's Disease. *Brain Res.* **2020**, 1730, No. 146642.
- Nguyen, T. T.; Yoon, S.; Yang, Y.; Lee, H. B.; Oh, S.; Jeong, M. H.; Kim, J. J.; Yee, S. T.; Crişan, F.; Moon, C.; Lee, K. Y.; Kim, K. K.; Hur, J. S.; Kim, H.; Yang, C. Lichen Secondary Metabolites in Flavocetraria Cucullata Exhibit Anti-Cancer Effects on Human Cancer Cells through the Induction of Apoptosis and Suppression of Tumorigenic Potentials. *PLoS One* **2014**, 9 (10), No. e111575.
- Taş, İ.; Varlı, M.; Son, Y.; Han, J.; Kwak, D.; Yang, Y.; Zhou, R.; Gamage, C. D. B.; Pulat, S.; Park, S. Y.; Yu, Y. H.; Moon, K. S.; Lee, K. H.; Ha, H. H.; Hur, J. S.; Kim, H. Physciosporin Suppresses Mitochondrial Respiration, Aerobic Glycolysis, and Tumorigenesis in Breast Cancer. *Phytomedicine* **2021**, 91, No. 153674.
- Yang, Y.; Nguyen, T. T.; Jeong, M. H.; Crişan, F.; Yu, Y. H.; Ha, H. H.; Choi, K. H.; Jeong, H. G.; Jeong, T. C.; Lee, K. Y.; Kim, K. K.; Hur, J. S.; Kim, H. Inhibitory Activity of (+)-Usnic Acid against Non-Small Cell Lung Cancer Cell Motility. *PLoS One* **2016**, 11 (1), No. e0146575.
- Zhao, J.; Meyerkord, C. L.; Du, Y.; Khuri, F. R.; Fu, H. 14–3-3 Proteins as Potential Therapeutic Targets. *Semin Cell Dev Biol.* **2011**, 22 (7), 705–712.
- Zhou, Y.; Fu, X.; Guan, Y.; Gong, M.; He, K.; Huang, B. 1,3-Dicaffeoylquinic Acid Targeting 14–3-3 Tau Suppresses Human Breast Cancer Cell Proliferation and Metastasis through IL6/JAK2/PI3K Pathway. *Biochem. Pharmacol.* **2020**, 172, No. 113752.
- Kim, H.; Han, J. R.; Park, J.; Oh, M.; James, S. E.; Chang, S.; Lu, Q.; Lee, K. Y.; Ki, H.; Song, W. J.; Kim, K. δ -Catenin-Induced Dendritic Morphogenesis: An Essential Role of P190RhoGEF Interaction through AKT1-Mediated Phosphorylation. *J. Biol. Chem.* **2008**, 283 (2), 977–987.
- He, Y.; Han, J. R.; Chang, O.; Oh, M.; James, S. E.; Lu, Q.; Seo, Y. W.; Kim, H.; Kim, K. 14–3-3 ϵ/ζ Affects the Stability of δ -Catenin and Regulates δ -Catenin-Induced Dendrogenesis. *FEBS Open Bio* **2013**, 3, 16–21.
- Young, G. M.; Radhakrishnan, V. M.; Centuori, S. M.; Gomes, C. J.; Martinez, J. D. Comparative Analysis of 14–3-3 Isoform Expression and Epigenetic Alterations in Colorectal Cancer. *BMC Cancer* **2015**, 15 (1), 1–10.
- Gardino, A. K.; Yaffe, M. B. 14–3-3 Proteins as Signaling Integration Points for Cell Cycle Control and Apoptosis. *Semin Cell Dev Biol.* **2011**, 22 (7), 688–695.
- Kleppe, R.; Martinez, A.; Døskeland, S. O.; Haavik, J. The 14–3-3 Proteins in Regulation of Cellular Metabolism. *Semin. Cell Dev. Biol.* **2011**, 22 (7), 713–719.
- Wang, B.; Yang, H.; Liu, Y. C.; Jelinek, T.; Zhang, L.; Ruoslahti, E.; Fu, H. Isolation of High-Affinity Peptide Antagonists of 14–3-3 Proteins by Phage Display. *Biochemistry* **1999**, 38 (38), 12499–12504.
- Petosa, C.; Masters, S. C.; Bankston, L. A.; Pohl, J.; Wang, B.; Fu, H.; Liddington, R. C. 14–3-3 ζ Binds a Phosphorylated Raf Peptide and an Unphosphorylated Peptide via Its Conserved Amphiphatic Groove. *J. Biol. Chem.* **1998**, 273 (26), 16305–16310.
- Stevens, L. M.; Sijbesma, E.; Botta, M.; MacKintosh, C.; Obsil, T.; Landrieu, I.; Cau, Y.; Wilson, A. J.; Karawajczyk, A.; Eickhoff, J.; Davis, J.; Hann, M.; O'Mahony, G.; Doveston, R. G.; Brunsveld, L.; Ottmann, C. Modulators of 14–3-3 Protein-Protein Interactions. *J. Med. Chem.* **2018**, 61 (9), 3755–3778.
- Layfield, R.; Fergusson, J.; Aitken, A.; Lowe, J.; Landon, M.; Mayer, R. J. Neurofibrillary Tangles of Alzheimer's Disease Brains Contain 14–3-3 Proteins. *Neurosci. Lett.* **1996**, 209 (1), 57–60.
- Sadik, G.; Tanaka, T.; Kato, K.; Yamamoto, H.; Nessa, B. N.; Morihara, T.; Takeda, M. Phosphorylation of Tau at Ser214 Mediates Its Interaction with 14–3-3 Protein: Implications for the Mechanism of Tau Aggregation. *J. Neurochem* **2009**, 108 (1), 33–43.
- Milroy, L. G.; Bartel, M.; Henen, M. A.; Leysen, S.; Adriaans, J. M. C.; Brunsveld, L.; Landrieu, I.; Ottmann, C. Stabilizer-Guided Inhibition of Protein-Protein Interactions. *Angew. Chem., Int. Ed.* **2015**, 54 (52), 15720–15724.
- Wu, H.; Ge, J.; Yao, S. Q. Microarray-Assisted High-Throughput Identification of a Cell-Permeable Small-Molecule Binder of 14–3-3 Proteins. *Angew. Chem.* **2010**, 122 (37), 6678–6682.
- Arrendale, A.; Kim, K.; Choi, J. Y.; Li, W.; Geahlen, R. L.; Borch, R. F. Synthesis of a Phosphoserine Mimetic Prodrug with Potent 14–3-3 Protein Inhibitory Activity. *Chem. Biol.* **2012**, 19 (6), 764–771.
- Corradi, V.; Mancini, M.; Manetti, F.; Petta, S.; Santucci, M. A.; Botta, M. Identification of the First Non-Peptidic Small Molecule Inhibitor of the c-Abl/14–3-3 Protein-Protein Interactions Able to Drive Sensitive and Imatinib-Resistant Leukemia Cells to Apoptosis. *Bioorg. Med. Chem. Lett.* **2010**, 20 (20), 6133–6137.
- Corradi, V.; Mancini, M.; Santucci, M. A.; Carlomagno, T.; Sanfelice, D.; Mori, M.; Vignaroli, G.; Falchi, F.; Manetti, F.; Radi, M.; Botta, M. Computational Techniques Are Valuable Tools for the Discovery of Protein-Protein Interaction Inhibitors: The 14–3-3 σ Case. *Bioorg. Med. Chem. Lett.* **2011**, 21 (22), 6867–6871.
- Mori, M.; Vignaroli, G.; Cau, Y.; Dinić, J.; Hill, R.; Rossi, M.; Colecchia, D.; Pešić, M.; Link, W.; Chiariello, M.; Ottmann, C.; Botta, M. Discovery of 14–3-3 Protein-Protein Interaction Inhibitors That

- Sensitize Multidrug-Resistant Cancer Cells to Doxorubicin and the Akt Inhibitor GSK690693. *ChemMedChem*. **2014**, *9* (5), 973–983.
- (33) Valensin, D.; Cau, Y.; Calandro, P.; Vignaroli, G.; Dello Iacono, L.; Chiariello, M.; Mori, M.; Botta, M. Molecular Insights to the Bioactive Form of BV02, a Reference Inhibitor of 14–3-3 σ Protein–Protein Interactions. *Bioorg. Med. Chem. Lett.* **2016**, *26* (3), 894–898.
- (34) An, S. S.; Askovich, P. S.; Zarebinski, T. I.; Ahn, K.; Peltier, J. M.; von Rechenberg, M.; Sahasrabudhe, S.; Fredberg, J. J. A Novel Small Molecule Target in Human Airway Smooth Muscle for Potential Treatment of Obstructive Lung Diseases: A Staged High-Throughput Biophysical Screening. *Respir. Res.* **2011**, *12* (1), 1–9.
- (35) Zhao, J.; Du, Y.; Horton, J. R.; Upadhyay, A. K.; Lou, B.; Bai, Y.; Zhang, X.; Du, L.; Li, M.; Wang, B.; Zhang, L.; Barbieri, J. T.; Khuri, F. R.; Cheng, X.; Fu, H. Discovery and Structural Characterization of a Small Molecule 14–3-3 Protein–Protein Interaction Inhibitor. *Proc. Natl. Acad. Sci. U. S. A.* **2011**, *108* (39), 16212–16216.
- (36) Kim, Y. C.; Camaioni, E.; Ziganshin, A. U.; Ji, X. d.; King, B. F.; Wildman, S. S.; Rychkov, A.; Yoburn, J.; Kim, H.; Mohanram, A.; Harden, T. K.; Boyer, J. L.; Burnstock, G.; Jacobson, K. A. Synthesis and Structure–Activity Relationships of Pyridoxal-6-Arylazo-5 α -Phosphate and Phosphonate Derivatives as P2 Receptor Antagonists A 2'-Chloro-5'-Sulfo Analog of PPADS (C 14 H 12 O 9 N 3 ClPSNa), a Vinyl Phosphonate Derivative (C 15 H 12 O 11 N 3 PS 2 Na 3), and a Naphthylazo Derivative (C 18 H 14 O 12 N 3 PS 2 Na). *Drug Dev Res.* **1998**, *45*, 52–66.
- (37) Takemoto, Y.; Watanabe, H.; Uchida, K.; Matsumura, K.; Nakae, K.; Tashiro, E.; Shindo, K.; Kitahara, T.; Imoto, M. Chemistry and Biology of Moverastins, Inhibitors of Cancer Cell Migration. *Produced by Aspergillus*. *Chem. Biol.* **2005**, *12* (12), 1337–1347.
- (38) Sawada, M.; Kubo, S. I.; Matsumura, K.; Takemoto, Y.; Kobayashi, H.; Tashiro, E.; Kitahara, T.; Watanabe, H.; Imoto, M. Synthesis and Anti-Migrative Evaluation of Moverastin Derivatives. *Bioorg. Med. Chem. Lett.* **2011**, *21* (5), 1385–1389.
- (39) Tashiro, E.; Imoto, M. Screening and Target Identification of Bioactive Compounds That Modulate Cell Migration and Autophagy. *Bioorg. Med. Chem.* **2016**, *24* (15), 3283–3290.
- (40) Kobayashi, H.; Ogura, Y.; Sawada, M.; Nakayama, R.; Takano, K.; Minato, Y.; Takemoto, Y.; Tashiro, E.; Watanabe, H.; Imoto, M. Involvement of 14–3-3 Proteins in the Second Epidermal Growth Factor-Induced Wave of Rac1 Activation in the Process of Cell Migration. *J. Biol. Chem.* **2011**, *286* (45), 39259–39268.
- (41) Thiel, P.; Röglin, L.; Meissner, N.; Hennig, S.; Kohlbacher, O.; Ottmann, C. Virtual Screening and Experimental Validation Reveal Novel Small-Molecule Inhibitors of 14–3-3 Protein – Protein Interactions. *Chem. Commun.* **2013**, *49* (76), 8468–8470.
- (42) Hu, G.; Cao, Z.; Xu, S.; Wang, W.; Wang, J. Revealing the Binding Modes and the Unbinding of 14–3-3 σ Proteins and Inhibitors by Computational Methods. *Sci. Rep.* **2015**, *5* (1), 1–13.
- (43) Bier, D.; Rose, R.; Bravo-Rodriguez, K.; Bartel, M.; Ramirez-Anguita, J. M.; Dutt, S.; Wilch, C.; Klärner, F. G.; Sanchez-Garcia, E.; Schrader, T.; Ottmann, C. Molecular Tweezers Modulate 14–3-3 Protein–Protein Interactions. *Nature Chemistry* **2013**, *5* (3), 234–239.
- (44) Marra, M.; Camoni, L.; Visconti, S.; Fiorillo, A.; Evidente, A. The Surprising Story of Fusicoccin: A Wilt-Inducing Phytotoxin, a Tool in Plant Physiology and a 14–3-3-Targeted Drug. *Biomolecules* **2021**, *Vol. 11*, Page 1393 **2021**, *11* (9), 1393.
- (45) Oecking, C.; Eckerskorn, C.; Weiler, E. W. The Fusicoccin Receptor of Plants Is a Member of the 14–3-3 Superfamily of Eukaryotic Regulatory Proteins. *FEBS Lett.* **1994**, *352* (2), 163–166.
- (46) Anders, C.; Higuchi, Y.; Koschinsky, K.; Bartel, M.; Schumacher, B.; Thiel, P.; Nitta, H.; Preisig-Müller, R.; Schlichthörl, G.; Renigunta, V.; Ohkanda, J.; Daut, J.; Kato, N.; Ottmann, C. A Semisynthetic Fusicoccane Stabilizes a Protein–Protein Interaction and Enhances the Expression of K⁺ Channels at the Cell Surface. *Chem. Biol.* **2013**, *20* (4), 583–593.
- (47) Bier, D.; Bartel, M.; Sies, K.; Halbach, S.; Higuchi, Y.; Haranosono, Y.; Brummer, T.; Kato, N.; Ottmann, C. Small-Molecule Stabilization of the 14–3-3/Gab2 Protein–Protein Interaction (PPI) Interface. *ChemMedChem*. **2016**, *11* (8), 911–918.
- (48) Parvatkar, P.; Kato, N.; Uesugi, M.; Sato, S. i.; Ohkanda, J. Intracellular Generation of a Diterpene–Peptide Conjugate That Inhibits 14–3-3-Mediated Interactions. *J. Am. Chem. Soc.* **2015**, *137* (50), 15624–15627.
- (49) Rose, R.; Erdmann, S.; Bovens, S.; Wolf, A.; Rose, M.; Hennig, S.; Waldmann, H.; Ottmann, C. Identification and Structure of Small-Molecule Stabilizers of 14–3-3 Protein–Protein Interactions. *Angew. Chem., Int. Ed.* **2010**, *49* (24), 4129–4132.
- (50) Richter, A.; Rose, R.; Hedberg, C.; Waldmann, H.; Ottmann, C. An Optimised Small-Molecule Stabiliser of the 14–3-3–PMA2 Protein–Protein Interaction. *Chem. - Eur. J.* **2012**, *18* (21), 6520–6527.
- (51) Sato, S.; Jung, H.; Nakagawa, T.; Pawlosky, R.; Takeshima, T.; Lee, W. R.; Sakiyama, H.; Laxman, S.; Wynn, R. M.; Tu, B. P.; MacMillan, J. B.; De Brabander, J. K.; Veech, R. L.; Uyeda, K. Metabolite Regulation of Nuclear Localization of Carbohydrate-Response Element-Binding Protein (ChREBP): Role of Amp as an Allosteric Inhibitor. *J. Biol. Chem.* **2016**, *291* (20), 10515–10527.
- (52) Varlı, M.; Lee, E. Y.; Yang, Y.; Zhou, R.; Taş, İ.; Pulat, S.; Gamage, C. D. B.; Park, S. Y.; Hur, J. S.; Nam, S. J.; Kim, H. 1'-O-Methyl-Averantin Isolated from the Endolichenic Fungus *Jackrogersella* Sp. EL001672 Suppresses Colorectal Cancer Stemness via Sonic Hedgehog and Notch Signaling. *Sci. Rep.* **2023**, *13*, 2811.
- (53) Yoon, H. E.; Kim, K. S.; Kim, I. Y. 14–3-3 η Inhibits Chondrogenic Differentiation of ATDC5 Cell. *Biochem. Biophys. Res. Commun.* **2011**, *406* (1), 59–63.
- (54) Jin, Y. H.; Kim, Y. J.; Kim, D. W.; Baek, K. H.; Kang, B. Y.; Yeo, C. Y.; Lee, K. Y. Sirt2 Interacts with 14–3-3 β/γ and down-Regulates the Activity of P53. *Biochem. Biophys. Res. Commun.* **2008**, *368* (3), 690–695.
- (55) Taş, İ.; Zhou, R.; Park, S. Y.; Yang, Y.; Gamage, C. D. B.; Son, Y. J.; Paik, M. J.; Kim, H. Inflammatory and Tumorigenic Effects of Environmental Pollutants Found in Particulate Matter on Lung Epithelial Cells. *Toxicology in Vitro* **2019**, *59*, 300–311.
- (56) Pulat, S.; Hillman, P. F.; Kim, S.; Asolkar, R. N.; Kim, H.; Zhou, R.; Taş, İ.; Gamage, C. D. B.; Varlı, M.; Park, S. Y.; Park, S. C.; Yang, I.; Shin, J.; Oh, D. C.; Kim, H.; Nam, S. J.; Fenical, W. Marinobazzanan, a Bazzanane-Type Sesquiterpenoid, Suppresses the Cell Motility and Tumorigenesis in Cancer Cells. *Mar Drugs* **2023**, *21* (3), 153.
- (57) Gamage, C. D. B.; Lee, K.; Park, S. Y.; Varlı, M.; Lee, C. W.; Kim, S. M.; Zhou, R.; Pulat, S.; Yang, Y.; Taş, İ.; Hur, J. S.; Kang, K. B.; Kim, H. Phthalides Isolated from the Endolichenic *Arthrinium* Sp. EL000127 Exhibits Antiangiogenic Activity. *AGS Omega* **2023**, *16*, 49.
- (58) Gamage, C. D. B.; Kim, J. H.; Yang, Y.; Taş, İ.; Park, S. Y.; Zhou, R.; Pulat, S.; Varlı, M.; Hur, J. S.; Nam, S. J.; Kim, H. Libertellenone T, a Novel Compound Isolated from Endolichenic Fungus, Induces G2/M Phase Arrest, Apoptosis, and Autophagy by Activating the ROS/JNK Pathway in Colorectal Cancer Cells. *Cancers* **2023**, *15* (2), 489.
- (59) RUBIO, M. P.; GERAGHTY, K. M.; WONG, B. H. C.; WOOD, N. T.; CAMPBELL, D. G.; MORRICE, N.; MACKINTOSH, C. 14–3-3-Affinity Purification of over 200 Human Phosphoproteins Reveals New Links to Regulation of Cellular Metabolism, Proliferation and Trafficking. *Biochem. J.* **2004**, *379* (2), 395–408.
- (60) Phan, L.; Chou, P. C.; Velazquez-Torres, G.; Samudio, I.; Parreno, K.; Huang, Y.; Tseng, C.; Vu, T.; Gully, C.; Su, C. H.; Wang, E.; Chen, J.; Choi, H. H.; Fuentes-Mattei, E.; Shin, J. H.; Shiang, C.; Grabiner, B.; Blonska, M.; Skerl, S.; Shao, Y.; Cody, D.; Delacerda, J.; Kingsley, C.; Webb, D.; Carlock, C.; Zhou, Z.; Hsieh, Y. C.; Lee, J.; Elliott, A.; Ramirez, M.; Bankson, J.; Hazle, J.; Wang, Y.; Li, L.; Weng, S.; Rizk, N.; Wen, Y. Y.; Lin, X.; Wang, H.; Wang, H.; Zhang, A.; Xia, X.; Wu, Y.; Habra, M.; Yang, W.; Puszta, L.; Yeung, S. C.; Lee, M. H. ARTICLE The Cell Cycle Regulator 14–3-3s Opposes and Reverses Cancer Metabolic Reprogramming. *Nat. Commun.* **2015**, *16* (6), 7530.
- (61) Munier, C. C.; Ottmann, C.; Perry, M. W. D. 14–3-3 Modulation of the Inflammatory Response. *Pharmacol. Res.* **2021**, *163*, No. 105236.
- (62) Pennington, K.; Chan, T.; Torres, M.; Andersen, J. The dynamic and stress-adaptive signaling hub of 14-3-3: emerging mechanisms of

regulation and context-dependent protein-protein interactions. *Oncogene* **2018**, *37*, 5587–5604.

(63) Li, F.; Wang, Y.; Zeller, K. I.; Potter, J. J.; Wonsey, D. R.; O'Donnell, K. A.; Kim, J. W.; Yustein, J. T.; Lee, L. A.; Dang, C. V. Myc Stimulates Nuclearly Encoded Mitochondrial Genes and Mitochondrial Biogenesis. *Mol. Cell. Biol.* **2005**, *25* (14), 6225–6234.

(64) Sun, Y.; Zhao, X.; ZHOU, Y.; Hu, Y. MiR-124, MiR-137 and MiR-340 Regulate Colorectal Cancer Growth via Inhibition of the Warburg Effect. *Oncol. Rep.* **2012**, *28* (4), 1346–1352.

(65) Kim, J. W.; Tchernyshyov, I.; Semenza, G. L.; Dang, C. V. HIF-1-Mediated Expression of Pyruvate Dehydrogenase Kinase: A Metabolic Switch Required for Cellular Adaptation to Hypoxia. *Cell Metab* **2006**, *3* (3), 177–185.

(66) Dowling, P.; Hughes, D. J.; Larkin, A. M.; Meiller, J.; Henry, M.; Meleady, P.; Lynch, V.; Pardini, B.; Naccarati, A.; Levy, M.; Vodicka, P.; Neary, P.; Clynes, M. Elevated Levels of 14–3-3 Proteins, Serotonin, Gamma Enolase and Pyruvate Kinase Identified in Clinical Samples from Patients Diagnosed with Colorectal Cancer. *Clin. Chim. Acta* **2015**, *441*, 133–141.

(67) Yaffe, M. B. How Do 14–3-3 Proteins Work? - Gatekeeper Phosphorylation and the Molecular Anvil Hypothesis. *FEBS Lett.* **2002**, *513* (1), 53–57.

(68) Tzivion, G.; Dobson, M.; Ramakrishnan, G. FoxO Transcription Factors; Regulation by AKT and 14–3-3 Proteins. *Biochimica et Biophysica Acta (BBA) - Molecular Cell Research* **2011**, *1813* (11), 1938–1945.

(69) Porter, G. W.; Khuri, F. R.; Fu, H. Dynamic 14–3-3/Client Protein Interactions Integrate Survival and Apoptotic Pathways. *Semin Cancer Biol.* **2006**, *16* (3), 193–202.

(70) Fan, X.; Cui, L.; Zeng, Y.; Song, W.; Gaur, U.; Yang, M. 14–3-3 Proteins Are on the Crossroads of Cancer, Aging, and Age-Related Neurodegenerative Disease. *Int. J. Mol. Sci.* **2019**, *20* (14), 3518.

(71) Wu, W.; Gou, H.; Dong, J.; Yang, X.; Zhao, Y.; Peng, H.; Chen, D.; Geng, R.; Chen, L.; Liu, J. Usnic Acid Inhibits Proliferation and Migration through ATM Mediated DNA Damage Response in RKO Colorectal Cancer Cell. *Curr. Pharm. Biotechnol* **2021**, *22* (8), 1129–1138.

(72) Galanty, A.; Koczurkiewicz, P.; Wnuk, D.; Paw, M.; Karnas, E.; Podolak, I.; Węgrzyn, M.; Borusiewicz, M.; Madeja, Z.; Czyż, J.; Michalik, M. Usnic Acid and Atranorin Exert Selective Cytostatic and Anti-Invasive Effects on Human Prostate and Melanoma Cancer Cells. *Toxicology in Vitro* **2017**, *40*, 161–169.

(73) Yang, Y.; Bae, W. K.; Lee, J. Y.; Choi, Y. J.; Lee, K. H.; Park, M. S.; Yu, Y. H.; Park, S. Y.; Zhou, R.; Taş, I.; Gamage, C.; Paik, M. J.; Lee, J. H.; Chung, I. J.; Kim, K. K.; Hur, J. S.; Kim, S. K.; Ha, H. H.; Kim, H. Potassium Usnate, a Water-Soluble Usnic Acid Salt, Shows Enhanced Bioavailability and Inhibits Invasion and Metastasis in Colorectal Cancer. *Sci. Rep.* **2018**, *8* (1), 1–11.

(74) Taş, İ.; Han, J.; Park, S. Y.; Yang, Y.; Zhou, R.; Gamage, C. D. B.; Van Nguyen, T.; Lee, J. Y.; Choi, Y. J.; Yu, Y. H.; Moon, K. S.; Kim, K. K.; Ha, H. H.; Kim, S. K.; Hur, J. S.; Kim, H. Physciosporin Suppresses the Proliferation, Motility and Tumourigenesis of Colorectal Cancer Cells. *Phytomedicine* **2019**, *56*, 10–20.

(75) Lu, J.; Guo, H.; Treekitkarmongkol, W.; Li, P.; Zhang, J.; Shi, B.; Ling, C.; Zhou, X.; Chen, T.; Chiao, P. J.; Feng, X.; Seewaldt, V. L.; Muller, W. J.; Sahin, A.; Hung, M. C.; Yu, D. 14–3-3ζ Cooperates with ErbB2 to Promote Ductal Carcinoma In Situ Progression to Invasive Breast Cancer by Inducing Epithelial-Mesenchymal Transition. *Cancer Cell* **2009**, *16* (3), 195–207.

(76) Liu, T. A.; Jan, Y. J.; Ko, B. S.; Liang, S. M.; Chen, S. C.; Wang, J.; Hsu, C.; Wu, Y. M.; Liou, J. Y. 14–3-3ε Overexpression Contributes to Epithelial-Mesenchymal Transition of Hepatocellular Carcinoma. *PLoS One* **2013**, *8* (3), No. e57968.

(77) Hou, Z.; Peng, H.; White, D. E.; Wang, P.; Lieberman, P. M.; Halazonetis, T.; Rauscher, F. J. 14–3-3 Binding Sites in the Snail Protein Are Essential for Snail-Mediated Transcriptional Repression and Epithelial-Mesenchymal Differentiation. *Cancer Res.* **2010**, *70* (11), 4385–4393.

(78) Wu, Y. J.; Jan, Y. J.; Ko, B. S.; Liang, S. M.; Liou, J. Y. Involvement of 14–3-3 Proteins in Regulating Tumor Progression of Hepatocellular Carcinoma. *Cancers* **2015**, *7* (2), 1022–1036.

(79) Singh, N.; Nambiar, D.; Kale, R. K.; Singh, R. P. Usnic Acid Inhibits Growth and Induces Cell Cycle Arrest and Apoptosis in Human Lung Carcinoma A549 Cells. *Nutr. Cancer* **2013**, *65* (Suppl 1), 36–43.

(80) Hermeking, H.; Benzinger, A. 14–3-3 Proteins in Cell Cycle Regulation. *Semin Cancer Biol.* **2006**, *16* (3), 183–192.

(81) Gómez-Suárez, M.; Gutiérrez-Martínez, I. Z.; Hernández-Trejo, J. A.; Hernández-Ruiz, M.; Suárez-Pérez, D.; Candelario, A.; Kamekura, R.; Medina-Contreras, O.; Schnoor, M.; Ortiz-Navarrete, V.; Villegas-Sepúlveda, N.; Parkos, C.; Nusrat, A.; Nava, P. 14–3-3 Proteins Regulate Akt Thr308 Phosphorylation in Intestinal Epithelial Cells. *Cell Death Differ.* **2016**, *23* (6), 1060–72.

(82) Zeng, C.; Zhang, Z.; Luo, W.; Wang, L.; Zhou, H.; Nie, C. JNK Initiates Beclin-1 Dependent Autophagic Cell Death against Akt Activation. *Exp. Cell Res.* **2022**, *414* (2), 113105.

(83) Tsuruta, F.; Sunayama, J.; Mori, Y.; Hattori, S.; Shimizu, S.; Tsujimoto, Y.; Yoshioka, K.; Masuyama, N.; Gotoh, Y. JNK Promotes Bax Translocation to Mitochondria through Phosphorylation of 14–3-3 Proteins. *EMBO J.* **2004**, *23* (8), 1889–1899.

(84) Pozuelo-Rubio, M. 14–3-3 Proteins Are Regulators of Autophagy. *Cells* **2012**, *1*, 754–773.

(85) Miyazaki, M.; McCarthy, J. J.; Esser, K. A. Insulin like Growth Factor-1-Induced Phosphorylation and Altered Distribution of Tuberos Sclerosis Complex (TSC)1/TSC2 in C2C12 Myotubes. *FEBS Journal* **2010**, *277* (9), 2180–2191.

(86) Cai, S. L.; Tee, A. R.; Short, J. D.; Bergeron, J. M.; Kim, J.; Shen, J.; Guo, R.; Johnson, C. L.; Kiguchi, K.; Walker, C. L. Activity of TSC2 Is Inhibited by AKT-Mediated Phosphorylation and Membrane Partitioning. *J. Cell Biol.* **2006**, *173* (2), 279–289.

(87) Song, Y.; Dai, F.; Zhai, D.; Dong, Y.; Zhang, J.; Lu, B.; Luo, J.; Liu, M.; Yi, Z. Usnic Acid Inhibits Breast Tumor Angiogenesis and Growth by Suppressing VEGFR2-Mediated AKT and ERK1/2 Signaling Pathways. *Angiogenesis* **2012**, *15* (3), 421–32.

(88) Chen, S.; Dobrovolsky, V. N.; Liu, F.; Wu, Y.; Zhang, Z.; Mei, N.; Guo, L. The Role of Autophagy in Usnic Acid-Induced Toxicity in Hepatic Cells. *Toxicol. Sci.* **2014**, *142* (1), 33–44.

(89) He, C.-L.; Bian, Y.-Y.; Xue, Y.; Liu, Z.-X.; Zhou, K.-Q.; Yao, C.-F.; Lin, Y.; Zou, H.-F.; Luo, F.-X.; Qu, Y.-Y.; Zhao, J.-Y.; Ye, M.-L.; Zhao, S.-M.; Xu, W. Pyruvate Kinase M2 Activates MTORC1 by Phosphorylating AKT1S1. *Sci. Rep.* **2016**, 21524 DOI: [10.1038/srep21524](https://doi.org/10.1038/srep21524).

(90) Chang, C. C.; Zhang, C.; Zhang, Q.; Sahin, O.; Wang, H.; Xu, J.; Xiao, Y.; Zhang, J.; Rehman, S. K.; Li, P.; Hung, M. C.; Behbod, F.; Yu, D. Upregulation of Lactate Dehydrogenase a by 14–3-3ζ Leads to Increased Glycolysis Critical for Breast Cancer Initiation and Progression. *Oncotarget* **2016**, *7* (23), 35270–83.

(91) Jiang, Q.; Zhang, X.; Dai, X.; Han, S.; Wu, X.; Wang, L.; Wei, W.; Zhang, N.; Xie, W.; Guo, J. S6K1-Mediated Phosphorylation of PDK1 Impairs AKT Kinase Activity and Oncogenic Functions. *Nature Communications* **2022** *13:1* **2022**, *13* (1), 1–14.

(92) Choi, Y.; Jeon, H.; Akin, J. W.; Curry, T. E.; Jo, M. The FOS/AP-1 Regulates Metabolic Changes and Cholesterol Synthesis in Human Periovarian Granulosa Cells. *Endocrinology* **2021**, *162* (9), 1–18.

(93) Wu, Z.; Nicoll, M.; Ingham, R. J. AP-1 Family Transcription Factors: A Diverse Family of Proteins That Regulate Varied Cellular Activities in Classical Hodgkin Lymphoma and ALCL. *Experimental Hematology & Oncology* **2021** *10:1* **2021**, *10* (1), 1–12.

(94) Li, S.; Janosch, P.; Tanji, M.; Rosenfeld, G. C.; Waymire, J. C.; Mischak, H.; Kolch, W.; Sedivy, J. M. Regulation of Raf-1 Kinase Activity by the 14–3-3 Family of Proteins. *EMBO J.* **1995**, *14* (4), 685–696.

(95) Dong, Y.; Liu, H. D.; Zhao, R.; Yang, C. Z.; Chen, X. Q.; Wang, X. H.; Lau, L. T.; Chen, J.; Yu, A. C. H. Ischemia Activates JNK/c-Jun/AP-1 Pathway to up-Regulate 14–3-3γ in Astrocyte. *J. Neurochem* **2009**, *109* (SUPPL. 1), 182–188.

(96) Bae, J. A.; Bae, W. K.; Kim, S. J.; Ko, Y. S.; Kim, K. Y.; Park, S. Y.; Yu, Y. H.; Kim, E. A.; Chung, I. J.; Kim, H.; Ha, H. H.; Kim, K. K. A New KSRP-Binding Compound Suppresses Distant Metastasis of Colorectal Cancer by Targeting the Oncogenic KITENIN Complex. *Mol. Cancer* **2021**, *20* (1), 1–24.

(97) Dovrat, S.; Caspi, M.; Zilberberg, A.; Lahav, L.; Firsow, A.; Gur, H.; Rosin-Arbesfeld, R. 14–3-3 and β -Catenin Are Secreted on Extracellular Vesicles to Activate the Oncogenic Wnt Pathway. *Mol. Oncol* **2014**, *8* (5), 894–911.

(98) Luo, W.; Hu, H.; Chang, R.; Zhong, J.; Knabel, M.; O’Meally, R.; Cole, R. N.; Pandey, A.; Semenza, G. L. Pyruvate Kinase M2 Is a PHD3-Stimulated Coactivator for Hypoxia-Inducible Factor 1. *Cell* **2011**, *145* (5), 732–744.

(99) Fan, Y.; Mao, R.; Yang, J. Protein Cell Protein Cell & Protein Cell NF-KB and STAT3 Signaling Pathways Collaboratively Link Inflammation to Cancer. *Protein Cell* **2013**, *3*, 176–185.

(100) Zhang, J.; Chen, F.; Li, W.; Xiong, Q.; Yang, M.; Zheng, P.; Li, C.; Pei, J.; Ge, F. 14–3-3 ζ Interacts with Stat3 and Regulates Its Constitutive Activation in Multiple Myeloma Cells. *PLoS One* **2012**, *7* (1), No. e29554.

(101) Lee, J.-J.; Lee, J.-S.; Cui, M. N.; Yun, H. H.; Kim, H. Y.; Lee, S. H.; Lee, J.-H. BIS targeting induces cellular senescence through the regulation of 14–3-3 zeta/STAT3/SKP2/p27 in glioblastoma cells. *Cell Death Dis* **2014**, *5*, No. e1537, DOI: 10.1038/cddis.2014.501.

(102) Ge, F.; Li, W. L.; Bi, L. J.; Tao, S. C.; Zhang, Z. P.; Zhang, X. E. Identification of Novel 14–3-3 Interacting Proteins by Quantitative Immunoprecipitation Combined with Knockdown (QUICK). *J. Proteome Res.* **2010**, *9* (11), 5848.

(103) Sun, T. X.; Li, M. Y.; Zhang, Z. H.; Wang, J. Y.; Xing, Y.; Ri, M.; Jin, C. H.; Xu, G. H.; Piao, L. X.; Jin, H. L.; Zuo, H. X.; Ma, J.; Jin, X. Usnic Acid Suppresses Cervical Cancer Cell Proliferation by Inhibiting PD-L1 Expression and Enhancing T-Lymphocyte Tumor-Killing Activity. *Phytother. Res.* **2021**, *35* (7), 3916–3935.

(104) Sakai, A.; Otani, M.; Miyamoto, A.; Yoshida, H.; Furuya, E.; Tanigawa, N. Identification of Phosphorylated Serine-15 and –82 Residues of HSPB1 in 5-Fluorouracil-Resistant Colorectal Cancer Cells by Proteomics. *J. Proteomics* **2012**, *75* (3), 806–818.